STEREO / IMPACT / LET: Solar Energetic Particle Intensities

Revision	Effective Date	Description of Changes
Baseline	09/28/2022	First release
Revision 1	03/31/2026	Formatting and minor corrections

1.1 Overview

The Low Energy Telescope (LET) is one of four sensors that make up the Solar Energetic Particle (SEP) instrument of the IMPACT investigation for NASA's STEREO mission. LET consists of a sensor system made up of an array of 14 solid-state detectors composed of 54 segments that are individually analyzed by custom Pulse Height Analysis System Integrated Circuits (PHASICs). The signals from four PHASIC chips in each LET are used by a Minimal Instruction Set Computer (MISC) to provide on-board particle identification of energetic particles from H through Ni in ~12 energy intervals at event rates of up to ~1000 events/sec.

The primary measurement goal of the LET instrument is to measure the composition, energy spectra, and time variations of solar energetic particles ranging from H to Ni. The energy range for oxygen extends from ~3 to 30 MeV/nucleon. Detailed documentation of the instrument design and science goals may be found in the instrument paper published in Space Science Reviews (SSR): Space Sci Rev (2008) 136: 285–3 (https://doi.org/10.1007/s11214-007-9288-x).

Figures 1 and 2 show the instrument cross-section and species-energy coverage.

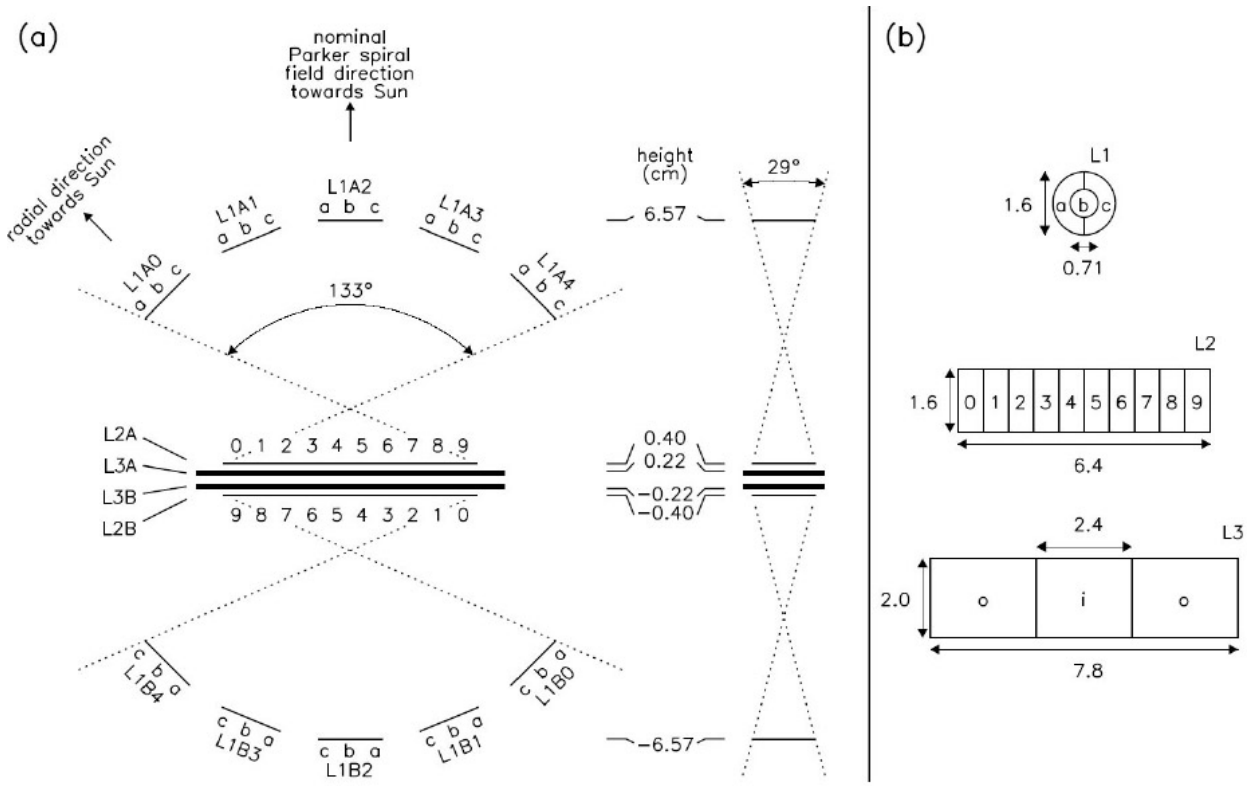

Figure 1:LET Instrument Cross-Section

Figure 2: LET Instrument Species and Energy-range. The diamonds represent the boundaries between energy bands.

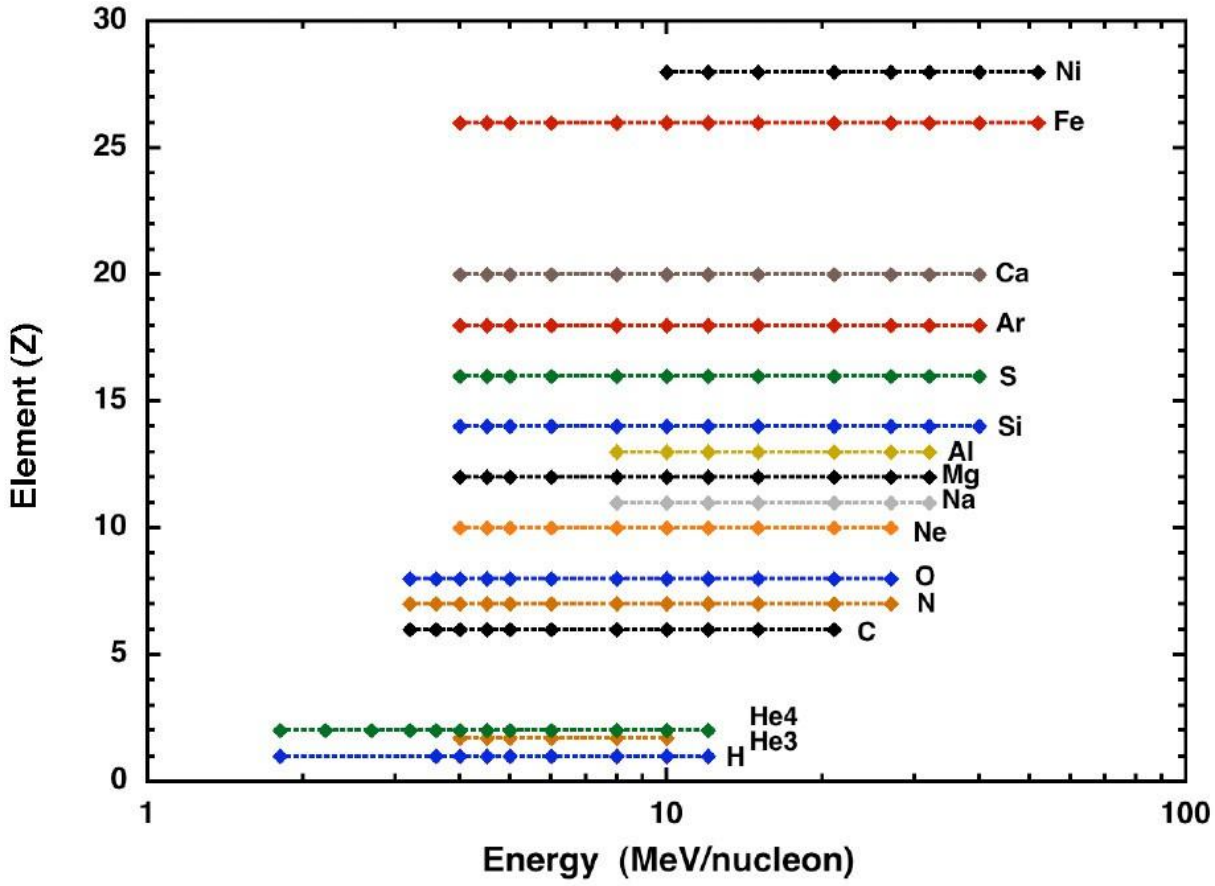

1.2 Heritage

The LET instrument employs the well-established dE/dx vs. total energy technique to determine the nuclear charge, and in some cases the mass, of detected heavy ions. This particle identification technique uses the energy loss signal from a detector that the particle fully penetrates (ΔE) and the energy deposited in a following detector in which the particle stops (E'), together with the thickness penetrated in the ΔE detector (L) to obtain an estimate of the particle's charge, Z. The technique has been used in many previous instruments, e.g. the SIS instrument on ACE, the CRS subsystem on Voyager, etc. The technique is described in detail in the SSR instrument paper, as is the implementation of this technique in the onboard particle identification system.

1.3 Instrument Data Acquisition and Onboard Data Processing Features

1.3.1 Dynamic Thresholds

An important feature of the onboard data acquisition is the "dynamic threshold" system. During large SEP events the single-detector count rates can increase by a factor of as much as 10^4, due mostly to low-energy protons. These elevated single-detector count rates create instrument dead-time and can also lead to chance coincidence events involving two separate particles. In order to minimize these effects,

the LET design includes “dynamic thresholds” in which the trigger threshold on selected detector segments are increased during periods when the count rates are high. This action reduces the count rates of selected detectors, minimizing dead-time and effectively reducing the geometry factor for H and He events with minimal effect on the geometry factor for heavy ions with Z ≥ 6.

The dynamic threshold state of the instrument is included in the raw telemetry and is required for conversion of the raw data to physical units. A detailed description of the dynamic threshold system is included in this document as Appendix 1.

1.3.2 Onboard Particle Identification and Energy/Sector Binning

See Appendix D, Section 2.4.

1.4 Level 1 and Level 2 Data Products Description

The LET Level 1 and Level 2 data are energetic particle intensities (1/(cm^2 s sr MeV/nuc)) for 16 species, in ~12 energy-bins per species.

The primary data access URL for the STEREO/LET data products during the active mission is the IMPACT/SEP instrument website at Caltech: https://izw1.caltech.edu/STEREO/index.html. The LET data web page is https://izw1.caltech.edu/STEREO/Level1/LET_public.html.

The Level 1 and Level 2 data are derived from the science and look-direction rates in the instrument telemetry data. These rates are described in detail in Appendix D, sections 2.4 and 2.5.

The highest time-resolution data provided by LET is 1 minute (Level 1 data). The LET 1-minute data are available in ASCII text format from Caltech, and in CDF format from the STEREO IMPACT Data portal at Berkeley, and from CDAWeb.

We also provide Level 2 data, which are 10-minute averaged, hourly-averaged, daily-averaged, and 27-day averaged data, derived directly from the 1-minute Level 1 data. These Level 2 data are in ASCII text files, with each file containing one calendar year of data, for one species, for one spacecraft. For the 10-minute averages, we also provide files containing 1 month of data.

Each ASCII file begins with a header that provides version and other provenance information and describes each data field.

The LET Level 1 and Level 2 data are available in three "flavors": Standard, Summed, and Sectored:

- **Standard**: Includes intensities for all the species/energy combinations defined in the LET onboard software. Some of the species/energy combinations may be set to FILL-DATA, as described in the release-notes/caveats. The latest release-notes/caveats are included in this document as Appendix 2.
- **Summed**: For each species the standard energy-bins are combined into wider energy-bins. These wider bins have better statistics and are common to most/all of the species identified by LET. These Summed data are useful for calculating element ratios and may be more useful than the Standard data during quiet periods.
- **Sectored**: The LET onboard software sorts events into 16 look-directions, or sectors (See Figure 3 and Appendix 3), 8 per side. Both the front (A-side) and rear (B-side) include particles from a 129deg x 29deg Field of View (FOV) with the 129deg fan looking along the ecliptic plane. The center of the A-side 129deg fan points at an angle that is 45deg from the Sun-spacecraft line. When the spacecraft is in its nominal roll orientation, this direction is 45deg west of the Sun

(along the average Parker Spiral direction at 1 AU), i.e., in the [-R,+T] direction. Since July 2015, after solar conjunction, the two STEREO spacecraft have been rolled 180deg about the Sun-spacecraft line in order to allow the high gain antenna to remain pointing at Earth. Consequently, the center of the A-side fan now points 45deg east of the Sun, in the [-R,-T] direction (i.e., perpendicular to the average Parker Spiral direction). Except for brief periods when the spacecraft is rolled for SECCHI or MAG calibrations, this will remain the case until the spacecraft passes by Earth again in 2023. Periods of off-nominal roll angles (including those at the beginning of the mission, when the spacecraft were still in Earth orbit) are shown in the plots at https://izw1.caltech.edu/STEREO/PLOTS/LET/AnisoPlots/pointingplot.pdf

For the sectored data in particular, it is important to understand the orientation of the LET instrument on the spacecraft, and the methods for calculating spacecraft attitude and roll angle. Detailed information for doing this is included in this document in Section 5.

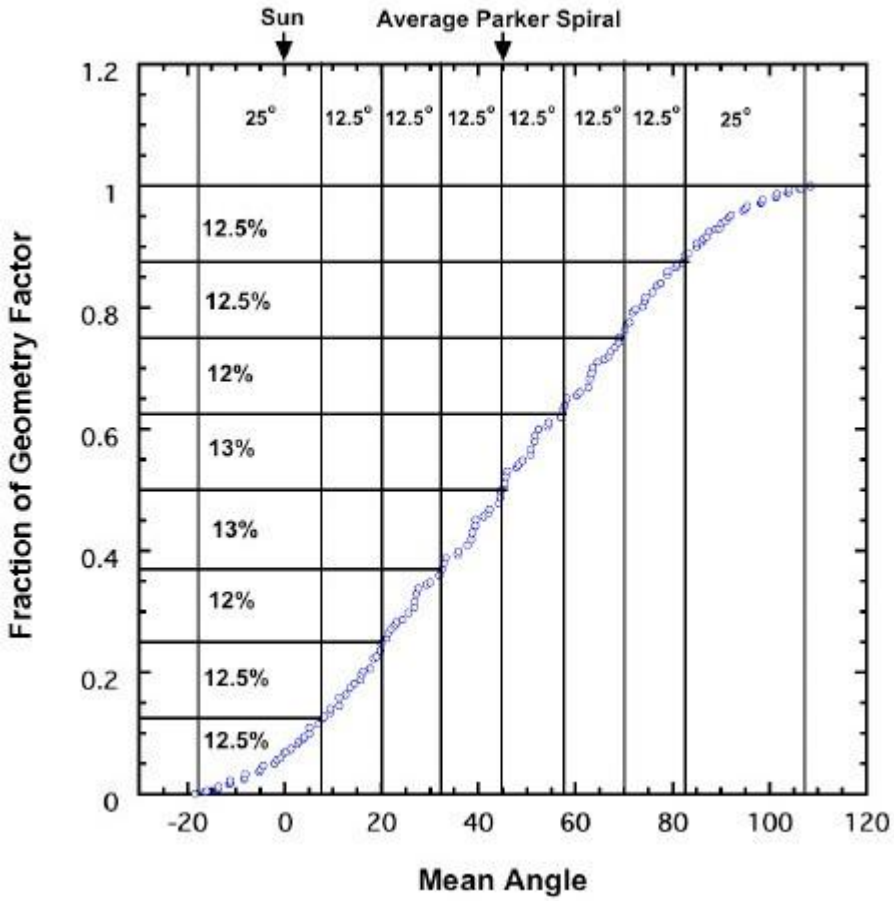

Figure 3: The LET viewing directions are divided into 8 sectors on the A-side and 8 on the B-side. Shown here is the fraction of the geometry factor in each sector on the A-side. In this representation the particles coming in a straight line from the Sun would arrive at 0 degrees and those arriving along the average Parker spiral angle would arrive at ~45 degrees. Note that the central six sectors are 12.5 degrees wide and the width of the two outside sectors is 25 degrees.

1.4.1 Full Listing of Standard Species/Energy Bins in the LET Level 1 and Level 2 data

```
H)
          1.8 -  2.2 MeV proton intensity (1/(cm^2 s sr MeV/nuc))
          2.2 -  2.7 MeV proton intensity (1/(cm^2 s sr MeV/nuc))
          2.7 -  3.2 MeV proton intensity (1/(cm^2 s sr MeV/nuc))
          3.2 -  3.6 MeV proton intensity (1/(cm^2 s sr MeV/nuc))
          3.6 -  4.0 MeV proton intensity (1/(cm^2 s sr MeV/nuc))
          4.0 -  4.5 MeV proton intensity (1/(cm^2 s sr MeV/nuc))
          4.5 -  5.0 MeV proton intensity (1/(cm^2 s sr MeV/nuc))
          5.0 -  6.0 MeV proton intensity (1/(cm^2 s sr MeV/nuc))
          6.0 -  8.0 MeV proton intensity (1/(cm^2 s sr MeV/nuc))
          8.0 - 10.0 MeV proton intensity (1/(cm^2 s sr MeV/nuc))
         10.0 - 12.0 MeV proton intensity (1/(cm^2 s sr MeV/nuc))
         12.0 - 15.0 MeV proton intensity (1/(cm^2 s sr MeV/nuc))
He3)
          2.2 -  2.7 MeV/n 3He intensity (1/(cm^2 s sr MeV/nuc))
          2.7 -  3.2 MeV/n 3He intensity (1/(cm^2 s sr MeV/nuc))
          3.2 -  3.6 MeV/n 3He intensity (1/(cm^2 s sr MeV/nuc))
          3.6 -  4.0 MeV/n 3He intensity (1/(cm^2 s sr MeV/nuc))
          4.0 -  4.5 MeV/n 3He intensity (1/(cm^2 s sr MeV/nuc))
          4.5 -  5.0 MeV/n 3He intensity (1/(cm^2 s sr MeV/nuc))
          5.0 -  6.0 MeV/n 3He intensity (1/(cm^2 s sr MeV/nuc))
          6.0 -  8.0 MeV/n 3He intensity (1/(cm^2 s sr MeV/nuc))
          8.0 - 10.0 MeV/n 3He intensity (1/(cm^2 s sr MeV/nuc))
         10.0 - 12.0 MeV/n 3He intensity (1/(cm^2 s sr MeV/nuc))
         12.0 - 15.0 MeV/n 3He intensity (1/(cm^2 s sr MeV/nuc))
He4)
          1.8 -  2.2 MeV/n 4He intensity (1/(cm^2 s sr MeV/nuc))
          2.2 -  2.7 MeV/n 4He intensity (1/(cm^2 s sr MeV/nuc))
          2.7 -  3.2 MeV/n 4He intensity (1/(cm^2 s sr MeV/nuc))
          3.2 -  3.6 MeV/n 4He intensity (1/(cm^2 s sr MeV/nuc))
          3.6 -  4.0 MeV/n 4He intensity (1/(cm^2 s sr MeV/nuc))
          4.0 -  4.5 MeV/n 4He intensity (1/(cm^2 s sr MeV/nuc))
          4.5 -  5.0 MeV/n 4He intensity (1/(cm^2 s sr MeV/nuc))
          5.0 -  6.0 MeV/n 4He intensity (1/(cm^2 s sr MeV/nuc))
          6.0 -  8.0 MeV/n 4He intensity (1/(cm^2 s sr MeV/nuc))
          8.0 - 10.0 MeV/n 4He intensity (1/(cm^2 s sr MeV/nuc))
         10.0 - 12.0 MeV/n 4He intensity (1/(cm^2 s sr MeV/nuc))
         12.0 - 15.0 MeV/n 4He intensity (1/(cm^2 s sr MeV/nuc))
He)
          2.2 -  2.7 MeV/n He intensity (1/(cm^2 s sr MeV/nuc))
          2.7 -  3.2 MeV/n He intensity (1/(cm^2 s sr MeV/nuc))
          3.2 -  3.6 MeV/n He intensity (1/(cm^2 s sr MeV/nuc))
          3.6 -  4.0 MeV/n He intensity (1/(cm^2 s sr MeV/nuc))
          4.0 -  4.5 MeV/n He intensity (1/(cm^2 s sr MeV/nuc))
          4.5 -  5.0 MeV/n He intensity (1/(cm^2 s sr MeV/nuc))
          5.0 -  6.0 MeV/n He intensity (1/(cm^2 s sr MeV/nuc))
          6.0 -  8.0 MeV/n He intensity (1/(cm^2 s sr MeV/nuc))
          8.0 - 10.0 MeV/n He intensity (1/(cm^2 s sr MeV/nuc))
         10.0 - 12.0 MeV/n He intensity (1/(cm^2 s sr MeV/nuc))
         12.0 - 15.0 MeV/n He intensity (1/(cm^2 s sr MeV/nuc))
C)
          3.2 -  3.6 MeV/n carbon intensity (1/(cm^2 s sr MeV/nuc))
          3.6 -  4.0 MeV/n carbon intensity (1/(cm^2 s sr MeV/nuc))
          4.0 -  4.5 MeV/n carbon intensity (1/(cm^2 s sr MeV/nuc))
```

```
 4.5 -  5.0 MeV/n carbon intensity (1/(cm^2 s sr MeV/nuc))
 5.0 -  6.0 MeV/n carbon intensity (1/(cm^2 s sr MeV/nuc))
 6.0 -  8.0 MeV/n carbon intensity (1/(cm^2 s sr MeV/nuc))
 8.0 - 10.0 MeV/n carbon intensity (1/(cm^2 s sr MeV/nuc))
10.0 - 12.0 MeV/n carbon intensity (1/(cm^2 s sr MeV/nuc))
12.0 - 15.0 MeV/n carbon intensity (1/(cm^2 s sr MeV/nuc))
15.0 - 21.0 MeV/n carbon intensity (1/(cm^2 s sr MeV/nuc))
21.0 - 27.0 MeV/n carbon intensity (1/(cm^2 s sr MeV/nuc))
27.0 - 33.0 MeV/n carbon intensity (1/(cm^2 s sr MeV/nuc))
N)
 3.2 -  3.6 MeV/n nitrogen intensity (1/(cm^2 s sr MeV/nuc))
 3.6 -  4.0 MeV/n nitrogen intensity (1/(cm^2 s sr MeV/nuc))
 4.0 -  4.5 MeV/n nitrogen intensity (1/(cm^2 s sr MeV/nuc))
 4.5 -  5.0 MeV/n nitrogen intensity (1/(cm^2 s sr MeV/nuc))
 5.0 -  6.0 MeV/n nitrogen intensity (1/(cm^2 s sr MeV/nuc))
 6.0 -  8.0 MeV/n nitrogen intensity (1/(cm^2 s sr MeV/nuc))
 8.0 - 10.0 MeV/n nitrogen intensity (1/(cm^2 s sr MeV/nuc))
10.0 - 12.0 MeV/n nitrogen intensity (1/(cm^2 s sr MeV/nuc))
12.0 - 15.0 MeV/n nitrogen intensity (1/(cm^2 s sr MeV/nuc))
15.0 - 21.0 MeV/n nitrogen intensity (1/(cm^2 s sr MeV/nuc))
21.0 - 27.0 MeV/n nitrogen intensity (1/(cm^2 s sr MeV/nuc))
27.0 - 33.0 MeV/n nitrogen intensity (1/(cm^2 s sr MeV/nuc))
O)
 3.2 -  3.6 MeV/n oxygen intensity (1/(cm^2 s sr MeV/nuc))
 3.6 -  4.0 MeV/n oxygen intensity (1/(cm^2 s sr MeV/nuc))
 4.0 -  4.5 MeV/n oxygen intensity (1/(cm^2 s sr MeV/nuc))
 4.5 -  5.0 MeV/n oxygen intensity (1/(cm^2 s sr MeV/nuc))
 5.0 -  6.0 MeV/n oxygen intensity (1/(cm^2 s sr MeV/nuc))
 6.0 -  8.0 MeV/n oxygen intensity (1/(cm^2 s sr MeV/nuc))
 8.0 - 10.0 MeV/n oxygen intensity (1/(cm^2 s sr MeV/nuc))
10.0 - 12.0 MeV/n oxygen intensity (1/(cm^2 s sr MeV/nuc))
12.0 - 15.0 MeV/n oxygen intensity (1/(cm^2 s sr MeV/nuc))
15.0 - 21.0 MeV/n oxygen intensity (1/(cm^2 s sr MeV/nuc))
21.0 - 27.0 MeV/n oxygen intensity (1/(cm^2 s sr MeV/nuc))
27.0 - 33.0 MeV/n oxygen intensity (1/(cm^2 s sr MeV/nuc))
Ne)
 3.2 -  3.6 MeV/n neon intensity (1/(cm^2 s sr MeV/nuc))
 3.6 -  4.0 MeV/n neon intensity (1/(cm^2 s sr MeV/nuc))
 4.0 -  4.5 MeV/n neon intensity (1/(cm^2 s sr MeV/nuc))
 4.5 -  5.0 MeV/n neon intensity (1/(cm^2 s sr MeV/nuc))
 5.0 -  6.0 MeV/n neon intensity (1/(cm^2 s sr MeV/nuc))
 6.0 -  8.0 MeV/n neon intensity (1/(cm^2 s sr MeV/nuc))
 8.0 - 10.0 MeV/n neon intensity (1/(cm^2 s sr MeV/nuc))
10.0 - 12.0 MeV/n neon intensity (1/(cm^2 s sr MeV/nuc))
12.0 - 15.0 MeV/n neon intensity (1/(cm^2 s sr MeV/nuc))
15.0 - 21.0 MeV/n neon intensity (1/(cm^2 s sr MeV/nuc))
21.0 - 27.0 MeV/n neon intensity (1/(cm^2 s sr MeV/nuc))
27.0 - 33.0 MeV/n neon intensity (1/(cm^2 s sr MeV/nuc))
33.0 - 40.0 MeV/n neon intensity (1/(cm^2 s sr MeV/nuc))
Na)
 6.0 -  8.0 MeV/n sodium intensity (1/(cm^2 s sr MeV/nuc))
 8.0 - 10.0 MeV/n sodium intensity (1/(cm^2 s sr MeV/nuc))
10.0 - 12.0 MeV/n sodium intensity (1/(cm^2 s sr MeV/nuc))
12.0 - 15.0 MeV/n sodium intensity (1/(cm^2 s sr MeV/nuc))
15.0 - 21.0 MeV/n sodium intensity (1/(cm^2 s sr MeV/nuc))
21.0 - 27.0 MeV/n sodium intensity (1/(cm^2 s sr MeV/nuc))
27.0 - 33.0 MeV/n sodium intensity (1/(cm^2 s sr MeV/nuc))
```

```
          33.0 - 40.0 MeV/n sodium intensity (1/(cm^2 s sr MeV/nuc))
Mg)
           3.2 -  3.6 MeV/n magnesium intensity (1/(cm^2 s sr MeV/nuc))
           3.6 -  4.0 MeV/n magnesium intensity (1/(cm^2 s sr MeV/nuc))
           4.0 -  4.5 MeV/n magnesium intensity (1/(cm^2 s sr MeV/nuc))
           4.5 -  5.0 MeV/n magnesium intensity (1/(cm^2 s sr MeV/nuc))
           5.0 -  6.0 MeV/n magnesium intensity (1/(cm^2 s sr MeV/nuc))
           6.0 -  8.0 MeV/n magnesium intensity (1/(cm^2 s sr MeV/nuc))
           8.0 - 10.0 MeV/n magnesium intensity (1/(cm^2 s sr MeV/nuc))
          10.0 - 12.0 MeV/n magnesium intensity (1/(cm^2 s sr MeV/nuc))
          12.0 - 15.0 MeV/n magnesium intensity (1/(cm^2 s sr MeV/nuc))
          15.0 - 21.0 MeV/n magnesium intensity (1/(cm^2 s sr MeV/nuc))
          21.0 - 27.0 MeV/n magnesium intensity (1/(cm^2 s sr MeV/nuc))
          27.0 - 33.0 MeV/n magnesium intensity (1/(cm^2 s sr MeV/nuc))
          33.0 - 40.0 MeV/n magnesium intensity (1/(cm^2 s sr MeV/nuc))
          40.0 - 52.0 MeV/n magnesium intensity (1/(cm^2 s sr MeV/nuc))
Al)
           6.0 -  8.0 MeV/n aluminum intensity (1/(cm^2 s sr MeV/nuc))
           8.0 - 10.0 MeV/n aluminum intensity (1/(cm^2 s sr MeV/nuc))
          10.0 - 12.0 MeV/n aluminum intensity (1/(cm^2 s sr MeV/nuc))
          12.0 - 15.0 MeV/n aluminum intensity (1/(cm^2 s sr MeV/nuc))
          15.0 - 21.0 MeV/n aluminum intensity (1/(cm^2 s sr MeV/nuc))
          21.0 - 27.0 MeV/n aluminum intensity (1/(cm^2 s sr MeV/nuc))
          27.0 - 33.0 MeV/n aluminum intensity (1/(cm^2 s sr MeV/nuc))
          33.0 - 40.0 MeV/n aluminum intensity (1/(cm^2 s sr MeV/nuc))
          40.0 - 52.0 MeV/n aluminum intensity (1/(cm^2 s sr MeV/nuc))

Si)
           3.2 -  3.6 MeV/n silicon intensity (1/(cm^2 s sr MeV/nuc))
           3.6 -  4.0 MeV/n silicon intensity (1/(cm^2 s sr MeV/nuc))
           4.0 -  4.5 MeV/n silicon intensity (1/(cm^2 s sr MeV/nuc))
           4.5 -  5.0 MeV/n silicon intensity (1/(cm^2 s sr MeV/nuc))
           5.0 -  6.0 MeV/n silicon intensity (1/(cm^2 s sr MeV/nuc))
           6.0 -  8.0 MeV/n silicon intensity (1/(cm^2 s sr MeV/nuc))
           8.0 - 10.0 MeV/n silicon intensity (1/(cm^2 s sr MeV/nuc))
          10.0 - 12.0 MeV/n silicon intensity (1/(cm^2 s sr MeV/nuc))
          12.0 - 15.0 MeV/n silicon intensity (1/(cm^2 s sr MeV/nuc))
          15.0 - 21.0 MeV/n silicon intensity (1/(cm^2 s sr MeV/nuc))
          21.0 - 27.0 MeV/n silicon intensity (1/(cm^2 s sr MeV/nuc))
          27.0 - 33.0 MeV/n silicon intensity (1/(cm^2 s sr MeV/nuc))
          33.0 - 40.0 MeV/n silicon intensity (1/(cm^2 s sr MeV/nuc))
          40.0 - 52.0 MeV/n silicon intensity (1/(cm^2 s sr MeV/nuc))
S)
           3.6 -  4.0 MeV/n sulfur intensity (1/(cm^2 s sr MeV/nuc))
           4.0 -  4.5 MeV/n sulfur intensity (1/(cm^2 s sr MeV/nuc))
           4.5 -  5.0 MeV/n sulfur intensity (1/(cm^2 s sr MeV/nuc))
           5.0 -  6.0 MeV/n sulfur intensity (1/(cm^2 s sr MeV/nuc))
           6.0 -  8.0 MeV/n sulfur intensity (1/(cm^2 s sr MeV/nuc))
           8.0 - 10.0 MeV/n sulfur intensity (1/(cm^2 s sr MeV/nuc))
          10.0 - 12.0 MeV/n sulfur intensity (1/(cm^2 s sr MeV/nuc))
          12.0 - 15.0 MeV/n sulfur intensity (1/(cm^2 s sr MeV/nuc))
          15.0 - 21.0 MeV/n sulfur intensity (1/(cm^2 s sr MeV/nuc))
          21.0 - 27.0 MeV/n sulfur intensity (1/(cm^2 s sr MeV/nuc))
          27.0 - 33.0 MeV/n sulfur intensity (1/(cm^2 s sr MeV/nuc))
          33.0 - 40.0 MeV/n sulfur intensity (1/(cm^2 s sr MeV/nuc))
          40.0 - 52.0 MeV/n sulfur intensity (1/(cm^2 s sr MeV/nuc))
Ar)
           3.6 -  4.0 MeV/n argon intensity (1/(cm^2 s sr MeV/nuc))
```

```
             4.0 -  4.5 MeV/n argon intensity (1/(cm^2 s sr MeV/nuc))
             4.5 -  5.0 MeV/n argon intensity (1/(cm^2 s sr MeV/nuc))
             5.0 -  6.0 MeV/n argon intensity (1/(cm^2 s sr MeV/nuc))
             6.0 -  8.0 MeV/n argon intensity (1/(cm^2 s sr MeV/nuc))
             8.0 - 10.0 MeV/n argon intensity (1/(cm^2 s sr MeV/nuc))
            10.0 - 12.0 MeV/n argon intensity (1/(cm^2 s sr MeV/nuc))
            12.0 - 15.0 MeV/n argon intensity (1/(cm^2 s sr MeV/nuc))
            15.0 - 21.0 MeV/n argon intensity (1/(cm^2 s sr MeV/nuc))
            21.0 - 27.0 MeV/n argon intensity (1/(cm^2 s sr MeV/nuc))
            27.0 - 33.0 MeV/n argon intensity (1/(cm^2 s sr MeV/nuc))
            33.0 - 40.0 MeV/n argon intensity (1/(cm^2 s sr MeV/nuc))
            40.0 - 52.0 MeV/n argon intensity (1/(cm^2 s sr MeV/nuc))
    Ca)
             3.6 -  4.0 MeV/n calcium intensity (1/(cm^2 s sr MeV/nuc))
             4.0 -  4.5 MeV/n calcium intensity (1/(cm^2 s sr MeV/nuc))
             4.5 -  5.0 MeV/n calcium intensity (1/(cm^2 s sr MeV/nuc))
             5.0 -  6.0 MeV/n calcium intensity (1/(cm^2 s sr MeV/nuc))
             6.0 -  8.0 MeV/n calcium intensity (1/(cm^2 s sr MeV/nuc))
             8.0 - 10.0 MeV/n calcium intensity (1/(cm^2 s sr MeV/nuc))
            10.0 - 12.0 MeV/n calcium intensity (1/(cm^2 s sr MeV/nuc))
            12.0 - 15.0 MeV/n calcium intensity (1/(cm^2 s sr MeV/nuc))
            15.0 - 21.0 MeV/n calcium intensity (1/(cm^2 s sr MeV/nuc))
            21.0 - 27.0 MeV/n calcium intensity (1/(cm^2 s sr MeV/nuc))
            27.0 - 33.0 MeV/n calcium intensity (1/(cm^2 s sr MeV/nuc))
            33.0 - 40.0 MeV/n calcium intensity (1/(cm^2 s sr MeV/nuc))
            40.0 - 52.0 MeV/n calcium intensity (1/(cm^2 s sr MeV/nuc))
    Fe)
             2.7 -  3.2 MeV/n iron intensity (1/(cm^2 s sr MeV/nuc))
             3.2 -  3.6 MeV/n iron intensity (1/(cm^2 s sr MeV/nuc))
             3.6 -  4.0 MeV/n iron intensity (1/(cm^2 s sr MeV/nuc))
             4.0 -  4.5 MeV/n iron intensity (1/(cm^2 s sr MeV/nuc))
             4.5 -  5.0 MeV/n iron intensity (1/(cm^2 s sr MeV/nuc))
             5.0 -  6.0 MeV/n iron intensity (1/(cm^2 s sr MeV/nuc))
             6.0 -  8.0 MeV/n iron intensity (1/(cm^2 s sr MeV/nuc))
             8.0 - 10.0 MeV/n iron intensity (1/(cm^2 s sr MeV/nuc))
            10.0 - 12.0 MeV/n iron intensity (1/(cm^2 s sr MeV/nuc))
            12.0 - 15.0 MeV/n iron intensity (1/(cm^2 s sr MeV/nuc))
            15.0 - 21.0 MeV/n iron intensity (1/(cm^2 s sr MeV/nuc))
            21.0 - 27.0 MeV/n iron intensity (1/(cm^2 s sr MeV/nuc))
            27.0 - 33.0 MeV/n iron intensity (1/(cm^2 s sr MeV/nuc))
            33.0 - 40.0 MeV/n iron intensity (1/(cm^2 s sr MeV/nuc))
            40.0 - 52.0 MeV/n iron intensity (1/(cm^2 s sr MeV/nuc))
            52.0 - 70.0 MeV/n iron intensity (1/(cm^2 s sr MeV/nuc))
    Ni)
             8.0 - 10.0 MeV/n nickel intensity (1/(cm^2 s sr MeV/nuc))
            10.0 - 12.0 MeV/n nickel intensity (1/(cm^2 s sr MeV/nuc))
            12.0 - 15.0 MeV/n nickel intensity (1/(cm^2 s sr MeV/nuc))
            15.0 - 21.0 MeV/n nickel intensity (1/(cm^2 s sr MeV/nuc))
            21.0 - 27.0 MeV/n nickel intensity (1/(cm^2 s sr MeV/nuc))
            27.0 - 33.0 MeV/n nickel intensity (1/(cm^2 s sr MeV/nuc))
            33.0 - 40.0 MeV/n nickel intensity (1/(cm^2 s sr MeV/nuc))
            40.0 - 52.0 MeV/n nickel intensity (1/(cm^2 s sr MeV/nuc))
            52.0 - 70.0 MeV/n nickel intensity (1/(cm^2 s sr MeV/nuc))
```

1.4.2 Full Listing of Summed Species/Energy Bins in the LET Level 1 and Level 2 data

```
    H)
```

```
            1.8 -  3.6 MeV proton intensity (1/(cm^2 s sr MeV/nuc))
            4.0 -  6.0 MeV proton intensity (1/(cm^2 s sr MeV/nuc))
            6.0 - 10.0 MeV proton intensity (1/(cm^2 s sr MeV/nuc))
           10.0 - 15.0 MeV proton intensity (1/(cm^2 s sr MeV/nuc))
He3)
            4.0 -  6.0 MeV/n 3He intensity (1/(cm^2 s sr MeV/nuc))
            6.0 - 10.0 MeV/n 3He intensity (1/(cm^2 s sr MeV/nuc))
           10.0 - 15.0 MeV/n 3He intensity (1/(cm^2 s sr MeV/nuc))
He4)
            1.8 -  3.6 MeV/n 4He intensity (1/(cm^2 s sr MeV/nuc))
            4.0 -  6.0 MeV/n 4He intensity (1/(cm^2 s sr MeV/nuc))
            6.0 - 10.0 MeV/n 4He intensity (1/(cm^2 s sr MeV/nuc))
           10.0 - 15.0 MeV/n 4He intensity (1/(cm^2 s sr MeV/nuc))
He)

            4.0 -  6.0 MeV/n He intensity (1/(cm^2 s sr MeV/nuc))
            6.0 - 10.0 MeV/n He intensity (1/(cm^2 s sr MeV/nuc))
           10.0 - 15.0 MeV/n He intensity (1/(cm^2 s sr MeV/nuc))
C)
            4.0 -  6.0 MeV/n carbon intensity (1/(cm^2 s sr MeV/nuc))
            6.0 - 10.0 MeV/n carbon intensity (1/(cm^2 s sr MeV/nuc))
           10.0 - 15.0 MeV/n carbon intensity (1/(cm^2 s sr MeV/nuc))
           15.0 - 27.0 MeV/n carbon intensity (1/(cm^2 s sr MeV/nuc))
N)
            4.0 -  6.0 MeV/n nitrogen intensity (1/(cm^2 s sr MeV/nuc))
            6.0 - 10.0 MeV/n nitrogen intensity (1/(cm^2 s sr MeV/nuc))
           10.0 - 15.0 MeV/n nitrogen intensity (1/(cm^2 s sr MeV/nuc))
           15.0 - 27.0 MeV/n nitrogen intensity (1/(cm^2 s sr MeV/nuc))
O)
            4.0 -  6.0 MeV/n oxygen intensity (1/(cm^2 s sr MeV/nuc))
            6.0 - 10.0 MeV/n oxygen intensity (1/(cm^2 s sr MeV/nuc))
           10.0 - 15.0 MeV/n oxygen intensity (1/(cm^2 s sr MeV/nuc))
           15.0 - 27.0 MeV/n oxygen intensity (1/(cm^2 s sr MeV/nuc))
Ne)
            4.0 -  6.0 MeV/n neon intensity (1/(cm^2 s sr MeV/nuc))
            6.0 - 10.0 MeV/n neon intensity (1/(cm^2 s sr MeV/nuc))
           10.0 - 15.0 MeV/n neon intensity (1/(cm^2 s sr MeV/nuc))
           15.0 - 27.0 MeV/n neon intensity (1/(cm^2 s sr MeV/nuc))
Na)
          10.0 - 15.0 MeV/n sodium intensity (1/(cm^2 s sr MeV/nuc))
          15.0 - 27.0 MeV/n sodium intensity (1/(cm^2 s sr MeV/nuc))
Mg)
            4.0 -  6.0 MeV/n magnesium intensity (1/(cm^2 s sr MeV/nuc))
            6.0 - 10.0 MeV/n magnesium intensity (1/(cm^2 s sr MeV/nuc))
           10.0 - 15.0 MeV/n magnesium intensity (1/(cm^2 s sr MeV/nuc))
           15.0 - 27.0 MeV/n magnesium intensity (1/(cm^2 s sr MeV/nuc))
Al)
            6.0 - 10.0 MeV/n aluminum intensity (1/(cm^2 s sr MeV/nuc))
           10.0 - 15.0 MeV/n aluminum intensity (1/(cm^2 s sr MeV/nuc))
           15.0 - 27.0 MeV/n aluminum intensity (1/(cm^2 s sr MeV/nuc))
Si)
            4.0 -  6.0 MeV/n silicon intensity (1/(cm^2 s sr MeV/nuc))
            6.0 - 10.0 MeV/n silicon intensity (1/(cm^2 s sr MeV/nuc))
           10.0 - 15.0 MeV/n silicon intensity (1/(cm^2 s sr MeV/nuc))
           15.0 - 27.0 MeV/n silicon intensity (1/(cm^2 s sr MeV/nuc))
           27.0 - 40.0 MeV/n silicon intensity (1/(cm^2 s sr MeV/nuc))
S)
            4.0 -  6.0 MeV/n sulfur intensity (1/(cm^2 s sr MeV/nuc))
```

```
                 6.0 - 10.0 MeV/n sulfur intensity (1/(cm^2 s sr MeV/nuc))
                10.0 - 15.0 MeV/n sulfur intensity (1/(cm^2 s sr MeV/nuc))
                15.0 - 27.0 MeV/n sulfur intensity (1/(cm^2 s sr MeV/nuc))
                27.0 - 40.0 MeV/n sulfur intensity (1/(cm^2 s sr MeV/nuc))
        Ar)
                 4.0 -  6.0 MeV/n argon intensity (1/(cm^2 s sr MeV/nuc))
                 6.0 - 10.0 MeV/n argon intensity (1/(cm^2 s sr MeV/nuc))
                10.0 - 15.0 MeV/n argon intensity (1/(cm^2 s sr MeV/nuc))
                15.0 - 27.0 MeV/n argon intensity (1/(cm^2 s sr MeV/nuc))
                27.0 - 40.0 MeV/n argon intensity (1/(cm^2 s sr MeV/nuc))
        Ca)
                 4.0 -  6.0 MeV/n calcium intensity (1/(cm^2 s sr MeV/nuc))
                 6.0 - 10.0 MeV/n calcium intensity (1/(cm^2 s sr MeV/nuc))
                10.0 - 15.0 MeV/n calcium intensity (1/(cm^2 s sr MeV/nuc))
                15.0 - 27.0 MeV/n calcium intensity (1/(cm^2 s sr MeV/nuc))
                27.0 - 40.0 MeV/n calcium intensity (1/(cm^2 s sr MeV/nuc))
        Fe)
                 4.0 -  6.0 MeV/n iron intensity (1/(cm^2 s sr MeV/nuc))
                 6.0 - 10.0 MeV/n iron intensity (1/(cm^2 s sr MeV/nuc))
                10.0 - 15.0 MeV/n iron intensity (1/(cm^2 s sr MeV/nuc))
                15.0 - 27.0 MeV/n iron intensity (1/(cm^2 s sr MeV/nuc))
                27.0 - 40.0 MeV/n iron intensity (1/(cm^2 s sr MeV/nuc))
        Ni)
                10.0 - 15.0 MeV/n nickel intensity (1/(cm^2 s sr MeV/nuc))
                15.0 - 27.0 MeV/n nickel intensity (1/(cm^2 s sr MeV/nuc))
                27.0 - 40.0 MeV/n nickel intensity (1/(cm^2 s sr MeV/nuc))
```

1.4.3 Full Listing of Sectored Species/Energy Bins in the LET Level 1 and Level 2 data

```
After Nov 22, 2010, the sectored rates are assigned as follows:
   0 -  15: H       4-6 MeV/nuc
  15 -  31: H       1.8-3.6
  32 -  47: 4He     4-6
  48 -  63: 4He     6-12
  64 -  79: CNO     4-6
  80 -  95: CNO     6-12
  96 - 111: NeMgSi  4-6
 112 - 127: NeMgSi  6-12
 128 - 143: Fe      4-12
 144 - 159: H       6-10

Prior to Nov 22, 2010 the sectored rates were:
   0 -  15: H       4-6 MeV/nuc
  15 -  31: 3He     4-6
  32 -  47: 4He     4-6
  48 -  63: 4He     6-12
  64 -  79: CNO     4-6
  80 -  95: CNO     6-12
  96 - 111: NeMgSi  4-6
 112 - 127: NeMgSi  6-12
 128 - 143: Fe      4-6
 144 - 159: Fe      6-12
```

1.4.4 Particle Intensity Calculation: Theoretical Description

The conversion from raw counts to energetic particle intensities uses the following simple formula:

- The raw data are counts (compressed), for N species, M energy bins, X look-directions. For STEREO/LET, N=16, M~12, X=16
- The physical quantity is Flux(N,M,X) (also called Intensity),

Where Flux(N,M,X) = counts(N,M,X)/Z,

Where Z = Livetime * Ebin_width(N,M,X) * Geom(N,M,X) *Eff(N,M,X)

Livetime is the amount of time for which the LET front-end electronics are "alive" and able to respond and read out data for instrument particle events. Except during periods of very high incident particle intensities, the livetime is close to 100% of the actual data accumulation time. The instrument livetime is monitored onboard and reported in the telemetry data.

Ebin_width is the width of the energy bin, in MeV/nucleon.

Geom is the Geometry factor (see Appendix 4). During large SEP events, the geometry factors for H and He depend upon the dynamic-threshold state of the instrument. This dynamic-threshold state is included in each record in the LET data and is used in the Level 1 data processing to select the appropriate geometry factor when computing the intensities.

Appropriate geometry factors for each dynamic-threshold state are included in the calibration files.

Eff is an efficiency factor, which is usually 1.0.

The steps involved in the computation of the intensities are:

- Read calibration data (Ebin_width, Geom, Eff arrays)
  - Note: these calibration data are time-dependent (several discreet changes were made early in the mission by the instrument team and these are described in the release notes in Appendix 2)
- Unpack data from CCSDS packets
- Read Livetime and dynamic-threshold state
- Decompress counts data - counts(N,M,X)
- Compute Flux(N,M,X)

The rates decompression is described in Appendix D.

The calibration data (Ebin_width, Geom, Eff arrays) are stored in ascii tables, and a separate table contains information about which calibration files to read based on the date/time of the data being processed.

The IDL code and associated calibration files that implement the above algorithm are available online from the STEREO IMPACT website at https://sprg.ssl.berkeley.edu/impact/peters/level1_software/

1.4.5 Error Analysis and Corrections

1.4.5.1 Uncertainties due to Counting Statistics

The Level 1 and Level 2 data contain the raw counts for item in the data products, for each time interval. The uncertainties due to counting statistics may be calculated by the user from these counts data using gaussian statistics (or poisson for low counts).

1.4.5.2 Systematic Uncertainties

1.4.5.2.1 Detector Thicknesses and Uniformity

Precise measurements of elemental and isotopic abundances require precise knowledge of thickness variations in the L1 and L2 detectors (L1 nominal thickness = 24 microns; L2 nominal thickness = 50 microns). Each of the ten L1 detectors has three segments. Each of two L2 detectors has 10 segments. Prior to final assembly thickness maps were made of all L1 detectors (3 equal-area segments) and L2 Detectors (10 equal-area segments). These maps were made with a collimated beam of 8.78 MeV alpha particles from a radioactive Th^{228} source. The most uniform devices were selected for flight. (Thermal vacuum data also played a role in detector selection.) Additional information on the L1, L2, and L3 thickness variations was available from accelerator data at the Michigan State University Cyclotron. The mean thicknesses of all LET L1 detectors in the LET-1 and LET-2 instruments are summarized in in Table 17 of the LET Instrument Paper in Space Science Reviews (Mewaldt et al. 2008). The thickness maps and trajectory corrections make it possible to do onboard identification of H, He, C, N, O, Ne, Mg, Si, S, Ar, Ca, Fe, and Ni, as well as ^{3}He and ^{4}He. The mass resolution of He in LET is 0.23 amu in Range 2 and 0.20 amu in Range 3.

1.4.5.2.2 Chance Coincidences

The segmentation of the L1, L2, and L3 detectors provides some protection against chance coincidences of two separate particles simulating a single event because it often will result in multiple hits in one of the layers. Range 3 ions will produce two independent measurements of the charge and energy which should agree. These checks can be made during ground processing. These issues are greater for electrons which often do not result in straight-line trajectories.

1.4.5.2.3 Livetime Effects

In the largest SEP events such as the July 23, 2012 event the livetime reported in telemetry by the flight software may be in error because of the extremely high count rates.

The onboard livetime counter records the amount of time that the instrument is waiting for a trigger. As soon as it gets a trigger, it system enters a coincidence window where it waits to see if any other detectors were hit. During this time, however, an independent event COULD get in and be analyzed by the instrument, even though the livetime counter does not recognize any portion of the coincidence window as "live". That is, to get the "proper" livetime, we need to add to the measured livetime the length of the coincidence window (or at least some fraction of it) for every instrument trigger. Since we record the number of triggers, NUMTRIG, this means we want:

NewLiveTime = Livetime + N * NUMTRIG,

where N is the length of time per trigger to be added.

N can be determined for LET by making use of the "livestim" data, which are events generated onboard by electronic pulses, and provide an independent measure of the livetime. Comparison of the livestim data with the reported livetime counter indicates that N = 0.9 microseconds.

In 2013, the Level 1 data processing software for LET was updated to implement this livetime correction, and the LET data from the start of the mission were reprocessed and rereleased on April 3, 2013 (See the Release Notes in Appendix 2).

1.4.5.2.4 Cross Calibration of the LET and HET Sensors with GOES and IMP-8

During December 2006 there was a series of large SEP events shortly after the launch of STEREO A&B. This period provided a rare opportunity to cross calibrate the STEREO LET & HET sensors with GOES. The first results of this cross calibration were presented in Mewaldt et al. (2015). They showed reasonable agreement for >10 MeV peak intensities and fluences. Subsequently Rodriguiz et al. (2017) cross-calibrated the proton response of GOES xx with both IMP-8 and STEREO A&B. The comparison showed that the GOES-15 was systematically overestimating proton intensities at higher energies (e.g., by x1.7 for >30 MeV; x2.1 for >60 MeV and x2.7 for >100 MeV protons. The results of this study also demonstrate good consistency between the two long-term IMP-8 GME and STEREO LET and HET solar proton data sets.

1.4.5.2.5 Quantifying the Systematic Uncertainties

Quantifying the contribution of these characteristics to a set of systematic errors is difficult. Some estimate can be derived from comparing LET measurements to those of other instruments (both on STEREO and other spacecraft such as ACE and GOES). Such comparisons have been made for individual SEP events (both large and small) at different times during the STEREO mission. These can be found in the following papers:

Cohen, C. M. S., Mason, G. M., Mewaldt, R. A., et al. 2008, Particle Acceleration and Transport in the Heliosphere and Beyond: 7th Annual International Astrophysics Conference, AIP, 1039, 118

Cohen, C. M. S., Luhmann, J. G., Mewaldt, R. A., et al. 2017a, Proceedings of 35th ICRC Conference, PoS(ICRC2017)134, 1

Cohen, C. M. S., Mason, G. M., & Mewaldt, R. A. 2017b, Astrophysical Journal, 843, 132

Mewaldt, R. A., Cohen, C. M. S., Cummings, A. C., et al. 2008, Proceedings of the 30th International Cosmic Ray Conference, 1, 107

Mewaldt, R. A., Leske, R. A., Stone, E. C., et al. 2009, Astrophysical Journal Letters, 693, L11

Wiedenbeck, M. E., Mason, G. M., Gómez-Herrero, R., et al. 2010, Twelfth International Solar Wind Conference. AIP Conference Proceedings,1216, 621

1.5 Calibration and Validation

The pre-flight and in-flight calibration of the STEREO LET instrument is described in detail in Section 4 of the LET instrument paper published in Space Science Reviews (SSR): Space Sci Rev (2008) 136: 285–3 (https://doi.org/10.1007/s11214-007-9288-x).

Pre-flight calibrations included:

- Electronic Pulser Calibrations

- Accelerator End-to-end Tests and Calibrations
- Radioactive Source Tests

The instrument was also calibrated in-flight early in the mission using in-flight particles. The stability of the detectors and electronics are monitored by checking whether the elements identified on-board remain centered in the bands in the three matrices as a function of time, temperature, and radiation dose (see Appendix D, Section 2.4). If not, it is possible to upload revised particle identification matrices, and this was done several times early in the mission. Large SEP events provide excellent statistical accuracy over a short time interval. Since the LET response overlaps with those of all three other SEP sensors, comparisons of the count rates, composition, and energy spectra between the four sensors make it possible to continually intercalibrate the SEP suite.

1.6 Higher Level Data Products

1.6.1 Proton Anisotropy Plots

These are yearly browse plots of LET 4-6 MeV proton sectored rates.

One of the products generated by the STEREO/LET instrument is particle rates measured in 16 different viewing directions, or sectors, distributed in two fans each spanning 133 degrees of longitude in the ecliptic and about 30-40 degrees of latitude out of the ecliptic, one pointing toward the Sun centered along the nominal Parker spiral direction and the other looking in the anti- Sun nominal field direction; see the LET instrument paper for more details (https://doi.org/10.1007/s11214-007-9288-x). These rates are available at various time resolutions in the "Sectored" directories from the LET data web page at Caltech (https://izw1.caltech.edu/STEREO/Public/LET_public.html).

The proton anisotropy browse plots serve as an aid to quickly determine when interesting periods with anisotropic particle intensities were detected by LET, or to help a user decide whether a period that may be interesting for other reasons (e.g., a large SEP event) showed detectable anisotropies in MeV ions. The user will need to download the sectored proton data to do a serious analysis, but these plots should help the user select which of these files to download.

The plots, and a full user guide with caveats and cautions, are available from the following URL:

https://izw1.caltech.edu/STEREO/PLOTS/LET/AnisoPlots/LETAnisoPlots.html

1.7 References

Mewaldt, R.A. et al, 2008, LET Instrument Paper: Space Science Reviews 136: 285–362 (https://doi.org/10.1007/s11214-007-9288-x).

Cohen, C. M. S., Mason, G. M., Mewaldt, R. A., et al. 2008, Particle Acceleration and Transport in the Heliosphere and Beyond: 7th Annual International Astrophysics Conference, AIP, 1039, 118

Cohen, C. M. S., Luhmann, J. G., Mewaldt, R. A., et al. 2017a, Proceedings of 35th ICRC Conference, PoS(ICRC2017)134, 1

Cohen, C. M. S., Mason, G. M., & Mewaldt, R. A. 2017b, Astrophysical Journal, 843, 132

Mewaldt, R. A., Cohen, C. M. S., Cummings, A. C., et al. 2008, Proceedings of the 30th International Cosmic Ray Conference, 1, 107

Mewaldt, R. A., Leske, R. A., Stone, E. C., et al. 2009, Astrophysical Journal Letters, 693, L11

Wiedenbeck, M. E., Mason, G. M., Gómez-Herrero, R., et al. 2010, Twelfth International Solar Wind Conference. AIP Conference Proceedings,1216, 621

Mewaldt et al, 2015, "A 360° survey of solar energetic particle events and one extreme event". Proceedings of 704 Science. PoS(ICRC2015)139. 34th International Cosmic Ray Conference, The Hague. (2015)

Rodriguiz, J.V. et al, 2017, "Validation of the Effect of Cross-Calibrated GOES Solar Proton Effective Energies on Derived Integral Fluxes by Comparison with STEREO Observations, J. V. Rodriguez, Space Weather

Appendix 1. Dynamic Thresholds

During large SEP events the single-detector count rates can increase by a factor of as much as 10^4 due mostly to low-energy protons. These elevated single-detector count rates create instrument dead-time and also lead to chance coincidence events involving two separate particles. In order to minimize these effects the LET design includes "dynamic thresholds" in which the trigger threshold on selected PHAs are increased during periods when the count rates are high. This action reduces the count rates of selected detectors, minimizing dead-time and effectively reducing the geometry factor for H and He events with minimal effect on the geometry factor for heavy ions with $Z \geq 6$.

The dynamic thresholds are implemented in a 3-stage process that is controlled by the summed count rates of those selected detectors that do not participate, as summarized in Table A1.1 and Figure A1.1. In the first stage, the high-gain ADCs (Analog to Digital Converters) on all 20 of the L1 outer segments are disabled. The effective threshold for triggering these devices is thereby raised from ~0.25 MeV to the low-gain thresholds, nominally set at 5 MeV. The result is that neither H nor He ions can trigger these higher thresholds except for particles incident at very wide angles (see Figure A1.2). As a result, the geometry factor for H and He is reduced by a factor of 5.

In the second stage the high-gain ADCs are disabled on all but the center L1s (L1A2 and L1B2), providing a decrease in the effective geometry factor for H and He by a second factor of ~5. At this point LET has reduced angular coverage for H and He (~90° coverage instead of ~130°), but the angular coverage for $Z \geq 6$ ions is not affected (except at the lowest and highest energies, where the L1 and L2 thresholds have some minor effects).

In the third stage the high-gain thresholds are disabled on all but the center two L2 segments on both the A and B sides (L2A4, L2A5, L2B4, L2B5 remain enabled), as well as the outside L3A and L3B segments. The nominal L2 and L3 low-gain thresholds are ~7 MeV and ~18 MeV, respectively, in order to be above the maximum energy loss of all but very wide-angle protons. This effectively reduces the geometry factor for H and He by an additional factor of ~4.5.

The monitor count rate for this process is the sum of all singles rates that are not affected by these changes (the centers of L1A2 and L1B2; L2A4, L2A5, L2B4, and L2B5; and the centers of L3A and L3B). These monitor-rate trigger levels may be changed by command; the nominal levels are summarized in Table A.1. In order to avoid toggling back and forth when the rates are near the trigger levels the dynamic thresholds for a given stage do not return to their nominal level until the count rates drop below the trigger level by some (commandable) factor (nominally = 2; see Table A.1). By disabling the high-gain thresholds the singles rates in a large event like those of 14 July 2000 (Bastille Day event) and 28 October 2003 will be reduced by a factor of ~10, with a corresponding increase in livetime (see Figure A.1). The state of the dynamic threshold currently implemented is indicated by two of the "miscellaneous bits" (Appendix 4, table 3.2) in the LET Science Data Frame, allowing the variable thresholds to be properly accounted for in calculating the true particle rates.

Table A1.1 Dynamic Threshold Trigger Levels and Geometry Factors

Affected Detectors	Trigger Rate (counts/s)	Turn-Off Rate (counts/s)	H and He Geometry Factor (cm^2sr)
L1 outsides	1000	500	0.807

L1 centers except L1A2 and L1B2	5000	2500	0.175
All L2s but L2A4, L2A5, L2B4, L2B5; L3 outsides	25,000	12,500	0.039

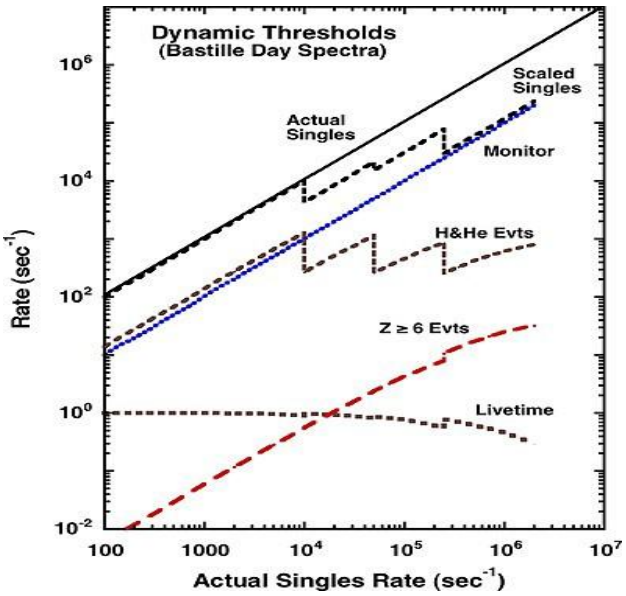

Fig. A1.1 Illustration of the effect of dynamic thresholds on the count rates and event readout from LET during a solar event with the composition and spectra of the July 14, 2000 (Bastille Day), SEP event. As the thresholds of various detector segments are gradually raised in response to the Monitor rate, the measured singles rate (labeled "scaled Singles") and the H and He event rates are reduced, thereby preserving instrument livetime to record a greater sample of $Z \geq 6$ events

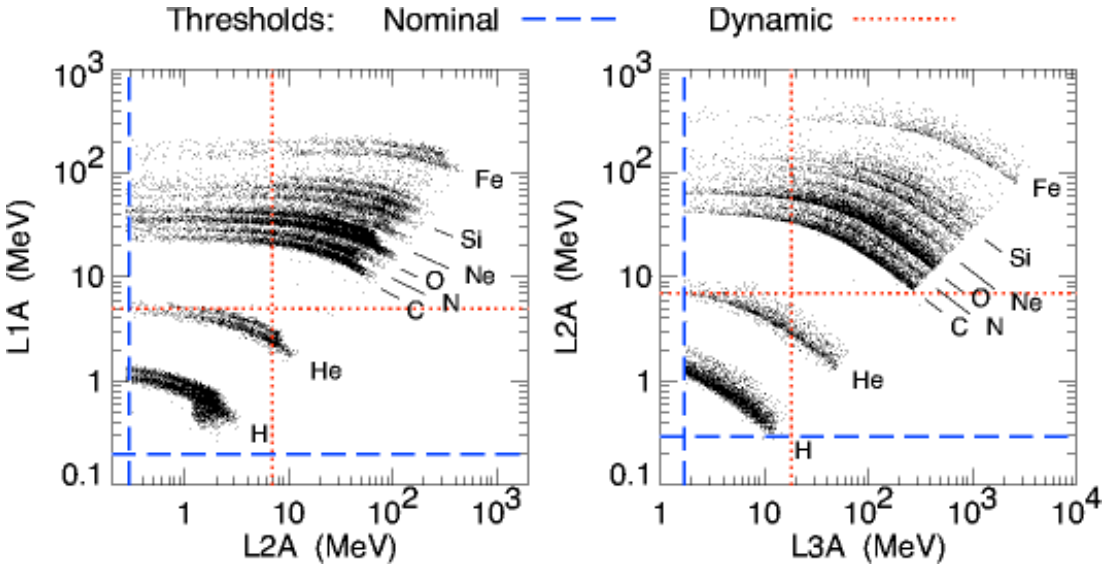

Fig. A1.2 Illustration of the nominal and dynamic thresholds for L1A•L2A events (*left panel*) and for L1A•L2A•L3A events (*right panel*)

Appendix 2. Release Notes and Caveats

Cumulative Release Notes for LET Level 1 data - Public data set.
See http://www.srl.caltech.edu/STEREO/docs/LET_Level1.html
for more LET Level 1 data documentation.

April 3, 2013: Important Update: Due to incorrect calculation of instrument livetimes in ground data processing, LET intensities at the peak of the July 23 2012 event were inaccurate. LET intensities during other periods of high particle intensities were also inaccurate to a lesser extent. We have corrected the livetime calculation, and a new version of the data has been released - Version 11.

Dec 3, 2012: Important Update: Due to incorrect calculation of instrument livetimes in ground data processing, LET intensities at the peak of the July 23 2012 event are inaccurate. We are working on a correction to the livetime calculation, and expect to reprocess these data soon.

April 16, 2012
The 15-21 MeV/nuc Carbon bin is not valid during high-rate periods (periods when the LET dynamic-threshold stats is >0). It is therefore set to "Fill data" for these periods.
The instrument thresholds are higher during these periods, and particles in this species-energy bin fall below the raised thresholds in some cases.

April 16, 2012
The total-energy calculation for particles that penetrate the instrument to Range 4 was found to be implemented incorrectly. The LET instruments on Ahead and Behind have been patched to correct the error.
LET Ahead was patched on April 16, 2012.
LET Behind was patched on April 18, 2012.
Prior to these dates, the following species-energy bands are invalid.
The LET data prior to the above patch dates are now reprocessed to replace the data in these bins with "FILL data".

```
 H: 12 - 15 *
4He: 12 - 15
 C: 21 - 27 *
 C: 27 - 33 *
 N: 21 - 27
 N: 27 - 33 *
 O: 27 - 33 *
Ne: 27 - 33 *
Ne: 33 - 40 *
Mg: 33 - 40 *
Mg: 40 - 52 *
Si: 33 - 40
Si: 40 - 52 *
Fe: 40 - 52
Fe: 52 - 70 *
```

Note: the species-energy bands marked with "*" above were already suppressed in the
Public data, for other reasons. So, this issue actually affects only 4 bands.

October 14, 2011
The LET instruments on Ahead and Behind have been patched to correct the instrument response when the instrument is in its "dynamic thresholds" mode

during high rate periods.
LET Behind was patched on October 11, 2011
LET Ahead was patched on October 14, 2011.
After these dates, the energy-bands for "heavies" that were invalid during high-rate periods
are now usable and are no longer being excluded from public release.

September 8, 2011
Due to unexpected changes in the LET instrument response when the instrument is in its
"dynamic thresholds" mode during high rate periods, we have replaced with "FILL data" the
data a subset of the energy-bands for for C, N, O, Ne, Na, Mg, AL, and Si, during high-rate
periods (approximately when 1.8-3.6 MeV proton intensities exceed ~150 counts/(cm^2 sr s MeV)).
We expect to upload a flight-software fix for this issue soon.
See Nov 11, 2010 note for more details of the issue.

November 22, 2010
We made some changes to the species represented in the LET sectored rates.
After Nov 22, 2010, the sectored rates are assigned as follows:

0 - 15:	H	4-6 MeV/nuc
15 - 31:	H	1.8-3.6
32 - 47:	4He	4-6
48 - 63:	4He	6-12
64 - 79:	CNO	4-6
80 - 95:	CNO	6-12
96 - 111:	NeMgSi	4-6
112 - 127:	NeMgSi	6-12
128 - 143:	Fe	4-12
144 - 159:	H	6-10

Prior to Nov 22, the rates were:

0 - 15:	H	4-6 MeV/nuc
15 - 31:	3He	4-6
32 - 47:	4He	4-6
48 - 63:	4He	6-12
64 - 79:	CNO	4-6
80 - 95:	CNO	6-12
96 - 111:	NeMgSi	4-6
112 - 127:	NeMgSi	6-12
128 - 143:	Fe	4-6
144 - 159:	Fe	6-12

November 11, 2010
Recently we have discovered some unexpected changes in the LET instrument response when the instrument is in its "dynamic thresholds" mode during high rate periods. During such periods, calibration shifts have been found that cause some counts for some elements to be mislabeled as the neighboring elements. At present, only ~4-10 MeV/nuc C, N, O, and Ne on the Behind spacecraft have been affected, and only during two time intervals during the SEP events of 2-3 August 2010 (day of year 214 and 215). Rates for these elements are inaccurate by perhaps as much as a factor of ~2

from approximately 6:41 through 14:44 on day 214 and again from 4:29 through 9:07 on day 215 of 2010. Until we can develop and implement commands to fix the problem (which we are working on), these errors will also recur during any similar high rate periods (approximately when 1.8-3.6 MeV proton intensities exceed ~150 counts/(cm^2 sr s MeV)) on both spacecraft in the future. Note that this problem does NOT affect the data during the large SEP events of December 2006 since the instruments were in a different mode at that time.

March 20, 2008
The geometry factors used to calculate intensities are under review. A new version of the LET Level 1 data will be released at some point in the future, using new geometry factors. The resulting changes from the current version will be on the order of 5%, or less.

Sept 4 2007
LET Level 1 software version 09.
Updated sectored geometry factors.

July 31, 2007
LET Level 1 software version 08.
First public data release.
See http://www.srl.caltech.edu/STEREO/docs/LET_Level1.html for more LET Level 1 documentation.

For the Public data set, we are currently flagging as bad the He data prior to March 29 2007, and the 3He data after March 29 2007. In addition, the following species/energy-bin channels are also flagged as bad in Public data set:
All Protons prior to the March 29 software uploads.
Protons below 4 MeV after the March 29 software uploads.
All 3He, for all time periods.
All 4He prior to the March 29 software uploads.
Fe below 5 MeV prior to the March 29 software uploads.
Fe below 4 MeV after the March 29 software uploads.
One or two energy-bins at the low and/or high ends for many species.

June 21 2007
LET Level 1 software version 08.
Added sectored data files.

June 14 2007
LET Level 1 software version 08.
This version includes the following changes from the previous version:
Added, Na, Al, S, Ar, Ca, Ni to output data files.

Added elemental helium.
After March 29, 2007, (at slightly different times on each spacecraft) events identified as 3He onboard are treated like 4He for energy-binning (a mass-number equal to 4 is used). This allows the 3He and 4He boxes to be combined on the ground to obtain elemental helium

```
        (He) intensities.  For data prior to the March 29 software uploads,
        the He data are FILL (-9999.9).
        For data after the March 29 software uploads, the 3He data are FILL.

        Improved software for reading in time-dependent factors files, and
        created new factors files for some time periods in Nov and Dec 2006
        when the instruments were in funny states.

        Added capability to flag each species/energy-bin channel as either
        "good" or "bad" for any time period. Bad channels are set to FILL.
        The flags for different time periods are stored as external tables,
        and the tables are read as needed depending on the time-stamp of the
        data being processed.

/home/stereo/LETL1Data/SRLonly/
    Factors_files/
    ReleaseNotes.txt
    ahead/
        2006/
            1Minute/
                Sectored/    (contains 1Minute-averaged ahead sectored daily
files for 2006)
                Standard/    (contains 1Minute ahead unsectored daily files
for 2006)
                Summed/      (contains 1Minute ahead summed energy-bin daily
files for 2006)

            10Minute/
                Sectored/    (contains 10Minute-averaged ahead sectored files
for 2006, with a month of data in each file)
                Standard/    (contains 10Minute-averaged ahead unsectored
files for 2006, with a month of data in each file)
                Summed/      (contains 10Minute-averaged ahead summed files
for 2006, with a year of month in each file)
            Hourly/
                Sectored/    (contains Hourly-averaged ahead sectored files
for 2006, with a year of data in each file)
                Standard/    (contains Hourly-averaged ahead unsectored files
for 2006, with a year of data in each file)
                Summed/      (contains Hourly-averaged ahead summed files for
2006, with a year of data in each file)
            Daily/
                Sectored/    (contains Daily-averaged ahead sectored files
for 2006, with a year of data in each file)
                Standard/    (contains Daily-averaged ahead unsectored files
for 2006, with a year of data in each file)
                Summed/      (contains Daily-averaged ahead summed files for
2006, with a year of data in each file)
        2007/ and so on...
    behind/
        Same organization as for ahead
```

Appendix 3. Pointing and Orbit Data for the SEP Instruments on the STEREO Spacecraft

This appendix provides information about orientation of the LET instrument on the STEREO Ahead and Behind spacecraft, and instructions for calculating pointing (attitude) and position vectors for any SEP instrument from the spacecraft ancillary data.

- Sections 1 and 2 deal with defining a LET coordinate system, and provide a recipe for converting vectors in the LET system to the spacecraft coordinate system. No recipe is provided for the other SEP instruments – this is left to the respective instrument teams.
- Section 3 describes a procedure for transforming pointing vectors in the spacecraft coordinate system to other useful coordinate systems, using transformation matrices provided by Caltech. These transformation matrices are provided in text data files, and the format of these files is described.
- Section 4 describes the format of the STEREO orbit data text files provided by Caltech.

3.1 LET Orientation with Respect to the Spacecraft Coordinate System

3.1.1 Both Spacecraft

For both spacecraft:

- LET is mounted on the S/C +Y panel.
- The S/C +X axis points sunward.
- During normal flight operations, the S/C X-Z plane and the ecliptic plane will generally be co-planar, approximately.

For both spacecraft, we define a LET coordinate system as follows:

- X: center of LET forward Field of View (FOV).
- Y: outward from spacecraft (same as S/C +Y axis).
- Z: completes the right-hand orthogonal set.

For the purposes of this discussion, we may ignore the fact that the origins of the LET and S/C origins are not co-located.

Note: the discussion below refers to the situation prior to the solar conjunction in 2015. Since July 2015, after solar conjunction, the two STEREO spacecraft have been rolled 180deg about the Sun-spacecraft line in order to allow the high gain antenna to remain pointing at Earth. Consequently, the center of the A-side fan now points 45deg east of the Sun, in the [-R,-T] direction (i.e., perpendicular to the average Parker Spiral direction).

3.1.2 Ahead Spacecraft

The Ahead S/C Y-axis points towards the north ecliptic pole. The LET X-Z plane is rotated $\theta = +45°$ about the S/C Y-axis (see Figure 1). To transform a vector $\mathbf{v}$ in the LET_a system to a vector $\mathbf{v'}$ in the S/C_a system,

$$\mathbf{v'} = T_a \mathbf{v}$$

$$\text{where } \mathbf{T_a} = \begin{bmatrix} \cos\theta & 0 & -\sin\theta \\ 0 & 1 & 0 \\ \sin\theta & 0 & \cos\theta \end{bmatrix}$$

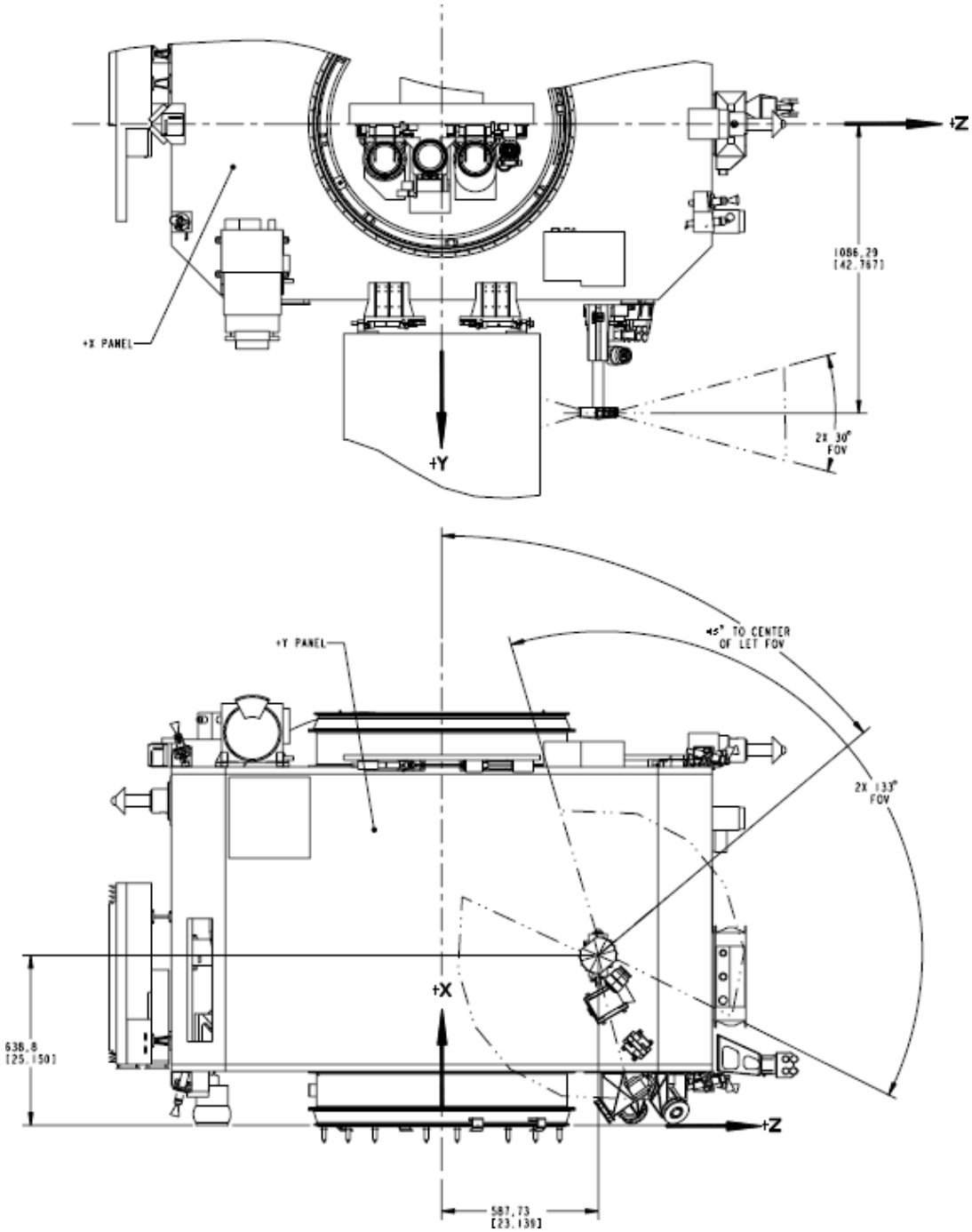

Figure A3.1: LET mounting and orientation on the Ahead Spacecraft, showing S/C X, Y, and Z axes. For illustration purposes only, positions and dimensions not exact.

3.1.3 Behind Spacecraft

The Behind S/C Y-axis points towards the south ecliptic pole. The LET is mounted in a different position on the S/C +Y panel, and the LET X-Z plane is rotated θ = -45° about the S/C Y-axis (note the negative angle). The transformation matrix to transform a vector **v** in the LET_b system to a vector **v′** in the S/C_b system is the same as for the Ahead S/C: just be sure to use the correct sign for the angle θ.

3.2 LET Sectors (Look Directions)

The various combinations of L1 and L2 segments define a total of 300 different directions in the LET X-Z plane. These directions are sorted during onboard data processing into sixteen sectors, defined in Table A3.1.

Table A3.1: LET Detector Combinations Sorted into Sectors

	L1A0			**L1A1**			**L1A2**			**L1A3**			**L1A4**		
	a	**b**	**c**	**a**	**b**	**c**	**a**	**b**	**c**	**a**	**b**	**c**	**a**	**b**	**c**
L2A0	6	5	5	3	3	3	2	1	1	0	0	0	0	0	0
L2A1	6	6	6	4	4	3	2	2	2	0	0	0	0	0	0
L2A2	7	6	6	5	4	4	3	2	2	1	1	0	0	0	0
L2A3	7	7	6	5	5	4	3	3	2	1	1	1	0	0	0
L2A4	7	7	7	6	5	5	4	3	3	2	1	1	0	0	0
L2A5	7	7	7	6	6	5	4	4	3	2	2	1	0	0	0
L2A6	7	7	7	6	6	6	5	4	4	3	2	2	1	0	0
L2A7	7	7	7	7	6	6	5	5	4	3	3	2	1	1	0
L2A8	7	7	7	7	7	7	5	5	5	4	3	3	1	1	1
L2A9	7	7	7	7	7	7	6	6	5	4	4	4	2	2	1

	L1B0			**L1B1**			**L1B2**			**L1B3**			**L1B4**		
	a	**b**	**c**	**a**	**b**	**c**	**a**	**b**	**c**	**a**	**b**	**c**	**a**	**b**	**c**
L2B0	14	13	13	11	11	11	10	9	9	8	8	8	8	8	8
L2B1	14	14	14	12	12	11	10	10	10	8	8	8	8	8	8
L2B2	15	14	14	13	12	12	11	10	10	9	9	8	8	8	8
L2B3	15	15	14	13	13	12	11	11	10	9	9	9	8	8	8
L2B4	15	15	15	14	13	13	12	11	11	10	9	9	8	8	8
L2B5	15	15	15	14	14	13	12	12	11	10	10	9	8	8	8
L2B6	15	15	15	14	14	14	13	12	12	11	10	10	9	8	8
L2B7	15	15	15	15	14	14	13	13	12	11	11	10	9	9	8
L2B8	15	15	15	15	15	15	12	13	13	12	11	11	9	9	9
L2B9	15	15	15	15	15	15	14	14	13	12	12	12	10	10	9

Each sector points in a direction defined by an angle with the LET +X axis. From this angle, the pointing vector for each sector may be calculated. The angles and pointing vectors (in the LET and the S/C coordinate systems) are listed in Table A3.2.

Table A3.2: LET Sector Pointing Vectors, in the LET and S/C coordinate systems.

Side	Sector	Angle with LET +X-axis (nominal)	Pointing Vector in LET coord.sys		Pointing Vector in Ahead S/C coord.sys		Pointing Vector in Behind S/C coord.sys	
			x	**z**	**x′**	**z′**	**x′**	**z′**
A	0	50	0.6428	0.7660	-0.0872	0.9962	0.9962	0.0872
A	1	31.25	0.8549	0.5188	0.2377	0.9713	0.9713	-0.2377
A	2	18.75	0.9469	0.3214	0.4423	0.8969	0.8969	-0.4423
A	3	6.25	0.9941	0.1089	0.6259	0.7799	0.7799	-0.6259
A	4	-6.25	0.9941	-0.1089	0.7799	0.6259	0.6259	-0.7799
A	5	-18.75	0.9469	-0.3214	0.8969	0.4423	0.4423	-0.8969
A	6	-31.25	0.8549	-0.5188	0.9713	0.2377	0.2377	-0.9713
A	7	-50	0.6428	-0.7660	0.9962	-0.0872	-0.0872	-0.9962
B	8	-130	-0.6428	-0.7660	0.0872	-0.9962	-0.9962	-0.0872
B	9	-148.75	-0.8549	-0.5188	-0.2377	-0.9713	-0.9713	0.2377
B	10	-161.25	-0.9469	-0.3214	-0.4423	-0.8969	-0.8969	0.4423
B	11	-173.75	-0.9941	-0.1089	-0.6259	-0.7799	-0.7799	0.6259
B	12	173.75	-0.9941	0.1089	-0.7799	-0.6259	-0.6259	0.7799
B	13	161.25	-0.9469	0.3214	-0.8969	-0.4423	-0.4423	0.8969
B	14	148.75	-0.8549	0.5188	-0.9713	-0.2377	-0.2377	0.9713
B	15	130	-0.6428	0.7660	-0.9962	0.0872	0.0872	0.9962

Note: The **y** component of all LET pointing vectors is zero, in both the LET and S/C coordinate systems.

Figure A3.2 below shows the coverage in longitudinal angle for each of the LET sectors.

The "Longitude from LET Axis" is the same angular measure as in column 3 of Table A3.2 above. Basically, the view cones are ~± 8 deg in the ecliptic and ~ ± 14° out of the ecliptic, except for the outside segments which are twice as wide. There are some variations from center to edge.

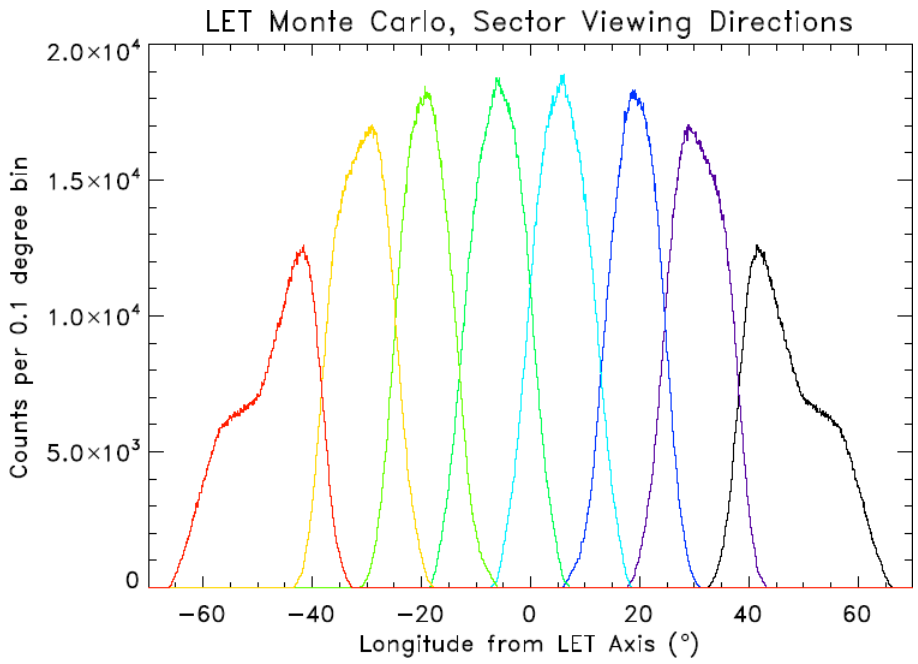

Figure A3.2: Coverage in longitudinal angle for each of the LET sectors.

3.3 Transformations from Spacecraft to Other Coordinate Systems

We have described the transformation of vectors from the LET to the S/C coordinate system. This section summarizes the procedures for transforming vectors in the S/C coordinate system to other useful coordinate systems.

The STEREO Science Center provides IDL SPICE software via the Solarsoft library that facilitates the transformation of vectors in the S/C coordinate system to other useful coordinate systems. The full list of supported coordinate systems and their descriptions may be found in the STEREO Solarsoft documentation. The subset currently assumed to be useful for LET data analysis is listed and described in Appendix B (more can be added as needed). The descriptions are copied from the STEREO Solarsoft documentation. Included are GEI, GSE, GSM, RTN, and several heliocentric coordinate systems.

Since a number of SEP team investigators either do not use IDL, or do not wish to install Solarsoft, Caltech provides text files containing transformation matrices for converting vectors from the S/C coordinate system to the coordinate systems listed in Appendix B. The format of each record in these files is as follows:

YYYY DoY Second Flag M_00 M_01 M_02 M_10 M_11 M_12 M_20 M_21 M_22

Where YYYY is the 4-digit year

DoY is the day-of-year (counting from 1)

Second is the second-of-day

Flag is 0 if the data are predictive

1 if the data are definitive

M_ij are the transformation matrix elements from the S/C coordinate system to the new coordinate system, where i is the row index, j is the column index.

The time cadence of records within these files is variable. A new record is appended only

- at the beginning of each day, **or**
- if the direction of the S/C X-axis changes by more than TOL degrees, **or**
- if the direction of the S/C Y-axis changes by more than TOL degrees

TOL is currently set to 0.25 degrees.

3.4 STEREO Orbit Data

The STEREO Science Center provides IDL SPICE software via the Solarsoft library that returns the coordinates of either of the two STEREO spacecraft in any of the supported coordinate systems. **Again, since a number of SEP team investigators either do not use IDL, or do not wish to install Solarsoft, Caltech provides text files containing position coordinates for the ahead and behind spacecraft in the coordinate systems listed in Appendix B (except for HGRTN/RTN) . The format of each record in these files is:**

YYYY DoY Second Flag P_0 P_1 P_2

Where YYYY is the 4-digit year

DoY is the day-of-year (counting from 1)

Second is the second-of-day

Flag is 0 if the data are predictive

1 if the data are definitive

P_i are the components of the spacecraft position vector in the given coordinate system.

The time cadence of records within these files is variable. A new record is appended only

- at the beginning of each day, **or**
- if the position of the S/C changes by more than TOL kilometers from the previous position.

TOL is currently set to 1000 km.

Transformation matrices for converting vectors from the S/C coordinate system to these coordinate systems are provided by Caltech as text files to the SEP instrument teams.

3.5 Coordinate Systems useful for LET Data Analysis

GEI: Geocentric Equatorial Inertial. The *X* axis points toward the first point of Aries (i.e. the vernal equinox), and the *Z* axis is aligned with the geographic north pole. When expressed in terms of longitude and latitude, this is the well known celestial coordinate system of right ascension and declination. This is realized with the J2000 ecliptic.

GSE: Geocentric Solar Ecliptic. *X* is the Earth-Sun line, and *Z* is aligned with the north pole for the ecliptic of date.

GSM: Geocentric Solar Magnetospheric. *X* is the Earth-Sun line, and *Z* is the projection of the north dipole axis.

H**CI: Heliocentric Inertial**. *Z* is the solar north rotational axis, and X is the solar ascending node on the J2000 ecliptic.

HEE: Heliocentric Earth Ecliptic. *X* is the Sun-Earth line, and *Z* is the north pole for the ecliptic of date.

HEEQ: Heliocentric Earth Equatorial. Z is the solar rotation axis, and X is in the plane containing the Z axis and Earth, at the intersection of the solar central meridian, and the heliographic equator. When converted to longitude and latitude, this is known as Stonyhurst heliographic coordinates. In FITS files, this coordinate system is abbreviated as "HEQ", so that variation is also recognized by the software.

HGRTN/RTN: Radial-Tangential-Normal. X axis points from Sun center to the spacecraft, and the Y axis is the cross product of the solar rotational axis and X, and lies in the solar equatorial plane (towards the West limb). For the STEREO Ahead spacecraft, this is realized through the dynamic coordinate frame STAHGRTN, while for STEREO Behind it is realized through STBHGRTN. When the Sun is used as the origin, the designation is HGRTN—with the spacecraft as origin, it's simply RTN.

Appendix 4. LET Geometry Factors

Note: these are nominal geometry factors. The calibration files used in Level 1 data processing may contain slightly different (updated) values.

Geometry Factor (cm2sr unit) of all combination of L1 vs. L2. 12/20/2006 AJD

	L1A0			L1A1			L1A2			L1A3			L1A4		
	a	b	c	a	b	c	a	b	c	a	b	c	a	b	c
L2A0	0.0328	0.0164	0.0275	0.0244	0.0114	0.0158	0.0157	0.0074	0.0128	0.0096	0.0044	0.0081	0.0056	0.0025	0.0044
L2A1	0.0267	0.0136	0.0264	0.0240	0.0116	0.0214	0.0173	0.0082	0.0150	0.0113	0.0053	0.0096	0.0067	0.0031	0.0055
L2A2	0.0212	0.0111	0.0224	0.0225	0.0111	0.0216	0.0186	0.0090	0.0168	0.0131	0.0062	0.0115	0.0081	0.0038	0.0068
L2A3	0.0168	0.0090	0.0185	0.0206	0.0103	0.0207	0.0193	0.0095	0.0183	0.0152	0.0073	0.0137	0.0100	0.0046	0.0084
L2A4	0.0133	0.0072	0.0151	0.0184	0.0095	0.0191	0.0196	0.0098	0.0193	0.0172	0.0083	0.0159	0.0124	0.0058	0.0106
L2A5	0.0106	0.0058	0.0124	0.0159	0.0083	0.0172	0.0193	0.0098	0.0196	0.0191	0.0095	0.0184	0.0151	0.0072	0.0133
L2A6	0.0084	0.0046	0.0100	0.0137	0.0073	0.0152	0.0183	0.0095	0.0193	0.0207	0.0103	0.0206	0.0185	0.0090	0.0168
L2A7	0.0068	0.0038	0.0081	0.0115	0.0062	0.0131	0.0168	0.0090	0.0186	0.0216	0.0111	0.0225	0.0224	0.0111	0.0212
L2A8	0.0055	0.0031	0.0067	0.0096	0.0053	0.0113	0.0150	0.0082	0.0173	0.0214	0.0116	0.0240	0.0264	0.0136	0.0267
L2A9	0.0044	0.0025	0.0056	0.0081	0.0044	0.0096	0.0128	0.0074	0.0157	0.0158	0.0114	0.0244	0.0275	0.0164	0.0328
Totals	0.1464	0.0770	0.1527	0.1687	0.0854	0.1650	0.1728	0.0876	0.1728	0.1650	0.0854	0.1687	0.1527	0.0770	0.1464

Dynamic Threshold State Geometry Factors (A-side and B-side combined)

State			
0	1	2	3
4.0473	0.8249	0.1752	0.0392

These factors do NOT take into account the detector combinations that are excluded in LET onboard processing for all range

State			
0	1	2	3
3.9972	0.8148	0.1752	0.0392

These factors DO take into account the detector combinations that are excluded in LET onboard processing for all Ranges

Notes: State 0: High-gain response fully enabled
State 1: High-gain response of all 20 L1 outer segments disabled
State 2: State 1 + disable high-gain response of 8 of 10 L1 center bulls-eyes (leaving only L1A2b and L1B2b enabled)
State 3: State 1 + State 2 + disable high-gain response of all L2s except L2A4, L2A5, L2B4, L2B5
Also disable L3 outer regions
These geometry factors apply only to H and He. Heavy ions trigger the low-gain PHAs, so they always have full geom factor.

Note: Geometry Factors for Sectored data are on Page 2

Geometry Factor (cm2sr unit) of all combination of L1 vs. I2.

	L1AO			L1A1			L1A2			L1A3			L1A4		
	a	b		a	b	c	a	b	c	a	b	c	a	b	c
L2AO							0.0157	0.0074	0.0128	0.0096	0.0044	0.0081	0.0000	00000	00000
L2A1				0240						0.0113	0.0053	0.0096	0.0067	0.0031	0.0055
L2A2				0.0225						0.0131	0.0062	0.0115	0.0081	0.0038	0.0068
L2A3				0.0206						0.0152	0.0073	0.0137	0.0100	0.0046	0.0084
L2A4		0.0072	0.0151							0.0172	0.0083	0.0159	0.0124	0.0058	0.0106
L2A5	0.0106	0.0058	0.0124									0.0184	0.0151	0.0072	0.0133
L2A6	0.0084	0.0046	0.0100									0.0206	0.0185	0.0090	0.0168
L2A7	0.0068	0.0038	0.0081										0.0224	0.0111	0.0212
L2A8	0.0055	0.0031	0.0067										0.0264	0.0136	0.0267
L2A9	0.0000	0.0000	0.0000	0.0081									0.0275	0.0164	0.0328
Totals	0.1420	0.0745	0.1471	0.1687	0.0854	0.1650	0.1728	0.0876	0.1728	0.1650	0.0854	0.1687	0.1471	0.0745	0.1420

ThesefactOfS DO take into account the detector combinations that are excluded in LET onboard processing for all Ranges
For B-side events, add8 to the A-side sector numbers to get the corresponding B-side sector number assigned by the onboard software.

Sector Geom Factors for Dynamic Threshold State O

Sector#						
0	1	2	3	4	5	6	7
0.2167	0.2627	0.2435	0.2765	0.2765	0.2435	0.2627	0.2167

Sector Geom Factors for Dynamic Threshold State 1: High.gain response of all 20 L1 outer segments disabled

Sector#						
0	1	2	3	4	5	6	7
0.0432	0.0539	0.0533	0.0534	0.0534	0.0533	0.0539	0.0432

Sector Geom Factors for Dynamic Threshold State 2: State 2: State 1 • disable high.gain response of 8 ol 1OL1 center bulls-e,.es (leaving only L1A2b and L1B2b enabled)

Sector#						
0		2	3	4	5	6	7
0.0000	0.0074	0.0171	0.0193	0.0193	0.0171	0.0074	0.0000

Sector Geom Factors for Dynamic Threshold State 3: State 2 • disable high-gain response of all I2s except I2A4, I2A5, L284, I2B5. Also outside L3A and L3B segments.

Sector#						
0	1	2	3	4	5	6	7
0.0000	0.0000	0.0000	0.0098	0.0098	0.0000	0.0000	0.0000

Thesegeometry factors apply only to Hand He. Heavy ions trigger the low.gain PHAs, so theyalways have full geom factor (As in State 0)

Appendix 5. LET Telemetry Data Format

The science data telemetry format document is included below as a reference (starting next page). For this appendix, the section numbering restarts at 1.

1. LET Science Data Frame Format

Allan Labrador (labrador@srl.caltech.edu), Caltech
9 April 2007 (Version 13.0)
(Slightly modified 8/30/07)
Updated 9/28/2022

1.0 Introduction

The purpose of this document is to describe the science data that will be transferred from the LET MISC to the SEP Central MISC. The format does not describe beacon data, nor does it describe CCSDS packet header or checksum information.

This document makes reference to information in the following external documents:

- LET Science Requirements Document
- *STEREO SEP LET and SEP Central: Flight Software Requirements* (*Version F, STEREO-CIT-002.F*)
- *STEREO IMPACT SEP Sensor Suite Commanding and Users Manual* (*Version F, STEREO-CIT-007.F*)
- *Specification of Functional Test Modules and In-flight Calibration Routines for LET* (*STEREO-CIT-006.A*)
- *STEREO/IMPACT LET Detector Naming* (*STEREO-CIT-0015.B*).
- *LET Software Counter Definitions* (*STEREO-CIT-019.A*).
- Interface Control Document (ICD) for the IMPACT Investigation.
- CCSDS 102.0-B-5 Packet Telemetry, Blue Book, Issue 5

Information is also included from other documents, memos, e-mail messages, discussion not in the formal STEREO/IMPACT document collection.

In this document, “LET Science Frame” and “LET Science Data Frame” may be used interchangeably.

2.0 LET Science Data Frame Format -- Requirements and Goals

The LET Science Data Frame Format is designed to accommodate the following LET Science requirements and goals, abstracted from the LET Science Requirements Document:

Table 1.1: Selected LET Science Requirements and Goals

	Requirements	**Goals**
Event (Pulse Height) Telemetry Rate	1 event/sec with prioritization	~4 events/sec with prioritization
Species Coverage (rates data)	10 species (H, 3He, 4He, C, N, O, Ne, Mg, Si, Fe)	16 species (H, 3He, 4He, C, N, O, Ne, Na, Mg, Al, Si, S, Ar, Ca, Fe, Ni)
Energy bins (rates data)	3 intervals for H 6 intervals for Z≥2	multiple energy bins, depending on species and penetration range
Event processing rate (rates data)	1000 events/sec	~5000 events/sec
Telemetry interval (time resolution) for rates data	15 minutes for all species	1 minute for all species

The LET Science Data Frame Format as described in this document will attempt to accommodate the rates-related Goals listed in Table 1.1.

The LET Science Data Frame Format is also designed with the following software engineering goals as guidance:

- Maximize bandwidth usage (i.e. minimize number of unused bits)
- Maximize event data (pulse height) bandwidth allocation
- Align data elements to nibble (4-bit) boundaries, byte boundaries, or MISC word (24-bit) boundaries, to simplify data examination in hexadecimal format
- Send data at short, regular intervals to the SEP Central MISC, to allow for faster debugging.
- In the event of bit errors (expected to be extremely rare), event data should be as reconstructible as possible to reduce the fraction of corrupted event data.

LET is allocated 16 CCSDS packets per minute, out of the 36 CCSDS packets per minute allocated to SEP. The 11 byte header and 1 byte checksum for each 272 byte CCSDS packet are not included in the LET Science Data Frame Format. Therefore, one minute of LET Science Data corresponds to 16*260 = 4160 bytes. Define these 16 CCSDS packets (minus headers and checksums) as one LET Science Data Frame, for transmission from LET to the SEP Central MISC. The goal is to accumulate and transmit all science rates (species counts) in one minute intervals, so that each LET Science Data Frame contains a complete set of science rates for a given minute.

According to the *SEP LET and Central MISC Processors Flight Software Requirements* document (Version E), the LET MISC will have opportunities to transmit complete CCSDS packets (with headers and checksum) to the SEP Central MISC once every three seconds. It is left to the SEP Central MISC to fill in time stamps and checksums in the CCSDS packets before passing them to the IDPU. The LET MISC will fill in ApIDs and source sequence counters and other pack identification information. A complete LET Science Frame is transmitted each minute, with rates and pulse heights having been packed into the Science Frame format and divided into CCSDS packets during the previous minute. If the event buffer (Section 2.8) does not get filled to the point of requiring the full 4160 byte allocation of the LET Science Frame, the LET MISC will fill the remaining packets with 0's.

The flow of data from LET to the IDPU is represented graphically in Figure 1.1.

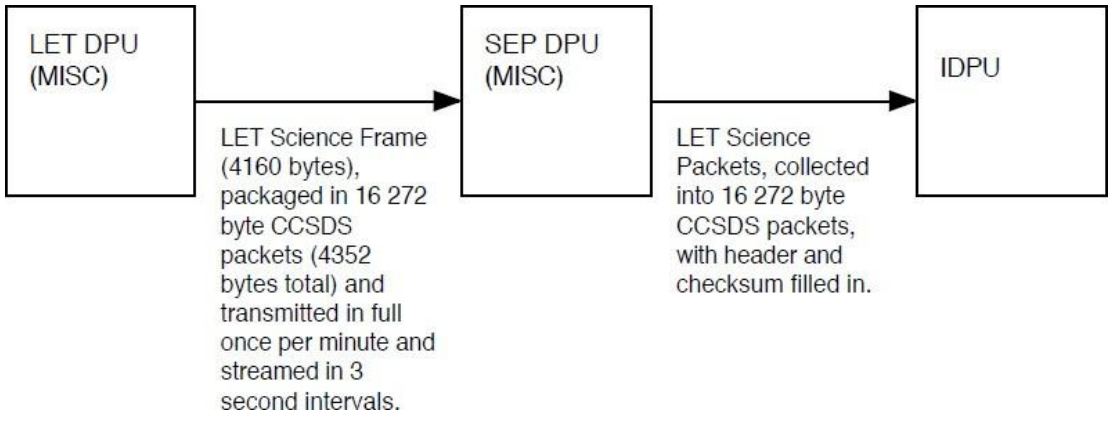

Figure 1.1: Data flow from LET to IDPU

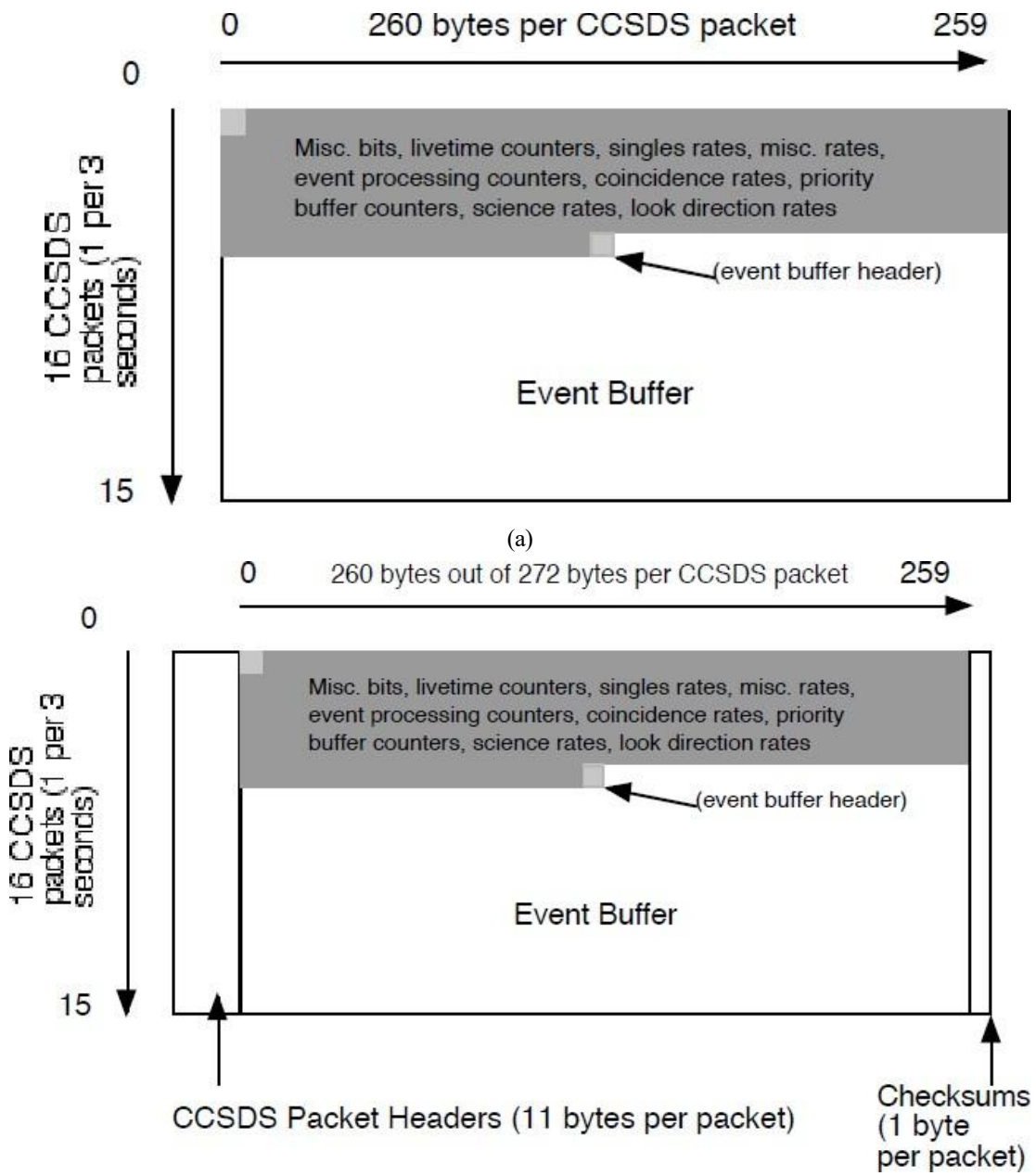

Figure 1.2: LET Science Frame Overview, (a) without CCSDS packet headers and checksums, and (b) with CCSDS packet headers and checksums. LET Science Frame Header is unlabeled at upper left. (Data elements not to horizontal scale.)

A LET Science Frame is shown graphically in Figure 1.2, with and without CCSDS packet headers and checksums. It includes 16 CCSDS packets for a total of 4160 bytes (not including CCSDS packet headers and checksums). Rates data occupy ~5.5 CCSDS packets. Event data occupy the remaining CCSDS packets.

Note that, although LET will be transmitting one science data packet every three seconds, only the first 16 of those packets will comprise a science frame. Within the science frame, unused event buffer space will be filled with 0's. The spare frames will also be filled with 0's and assigned a unique ApID.

2.1 Byte Order

The LET Science Frame is envisioned as an array of bytes or as a stream of bytes. Transmission of data elements is also envisioned as a stream of bytes. When a LET Science Frame element spans more than one byte, it will be transmitted high-byte-first. For example, Event Buffer Headers (Section 2.8) span four bytes, or one MISC word plus one byte, and these will be transmitted in the order of highest byte, second high byte, second low byte, and lowest byte.

2.2 ApID and Packet Number

The ApID value of 580 is assigned to every LET Science Frame Packet, and this value is stored in the CCSDS packet header (not part of the LET Science Frame itself). In order to identify individual packets within the LET Science Frame, bits 0–3 of the subseconds field of the CCSDS packet header are replaced by a packet number. The packet numbers are defined in Table 2.1, as also shown in Figure 1.2.

Table 2.1: LET Science Packet Numbers

Packet #	Packet Description
0–4	Science Frame Header, Counters and Rates
5	Counters and Rates, start of Event Buffer
6-15	Event Buffer frames

The ApID and packet numbers will be assigned by the LET MISC and entered into each CCSDS packet header. The LET Science Data Frame does not make direct use of the source sequence counter in each CCSDS packet header.

2.3 LET Science Frame Header

Some header information is included in the CCSDS packet headers (secondary headers). However, because CCSDS packet formatting may be removed during ground-based analysis in order to extract full LET Science data from each set of LET CCSDS packets, it will be useful to include a LET Science Frame Header.

The LET Science Frame Header is allocated as 5 bytes at the top of the LET Science Frame. Byte 0 is the spacecraft ID (SCID) and frame version number (SFVER). The two most significant bits are the spacecraft ID — 00 for the EM unit (no spacecraft), 01 for FM1 (the leading spacecraft, or "ahead"), and 10 for FM2 (the trailing spacecraft, or "behind"). The remaning bits are a LET Science Frame Version number; the current version number is 11. Should the version number ever exceed 128, the version number in these bits will be calculated modulo 128.

Bytes 1 and 2 (high byte and low byte – see Section 2.1) contain the number of valid bytes (SFLEN) in the complete LET Science Frame (not including CCSDS header and checksum). “Valid” bytes include all the bytes from the frame header to the last byte of the last event in the event buffer, and this counter does not include CCSDS packet headers or checksums. Because 6 CCSDS packets containing fixed format data are always present, this number is never less than 1418. This number never exceeds 4160. The three most significant bits of byte 1 are unused.

The last two bytes (bytes 3-4) of the LET Science Frame Header are defined as a checksum (SFCHECK, to verify the integrity of the LET Science Frame Data. The two bytes are set such that the sum of all bytes or MISC words modulo 2^{16} equal zero. Individual bytes are summed, with the checksum allowed to grow to 16 bits. This checksum is independent of the CCSDS packet checksums and is calculated by the LET MISC prior to the calculation of CCSDS packet checksums by SEP Central.

The contents of the LET Science Frame Header are summarized in Section 3.0.

2.4 Science rates (species counts, rate counters):

For the science rates coming with each frame, counts for H and He (He-3 and He-4), 13 heavy elements (C, N, O, Ne, Na, Mg, Al, Si, S, Ar, Ca, Fe, and Ni), and various "background" counts (including charge ranges) will be transmitted. Science Rates will be organized top–down in order of penetration range, then species, then energy. Science rates included in the LET Science Frame are summarized in Tables 3.9–3.14, and their locations in the LET Science Frame are detailed in the same tables.

As described in the *STEREO SEP LET and SEP Central Flight Software Requirements (Version F, STEREO–CIT–002.F)* document, particles which pass certain onboard processing cuts are sorted into matrices according to their penetration range in the instrument and by delta–E vs. E' measurements. Each matrix represents a penetration range — into the L2 detectors (RNG2, or L1L2), into one L3 detector (RNG3, or L2L3), or into two L3 detectors and possibly beyond (RNG4, PEN, or L3AL3B). Within each penetration range, the associated matrix covers a delta–E vs. E' space that spans particles from Z=1 (H) to Z≥40 (Zr). The matrices are used by onboard processing to identify particles by range in the instrument and charge, and further onboard processing is used to determine particle kinetic energy. The matrices span 128 bins in the x–axis and 400 bins in the y–axis, and they are shown graphically in Appendix C. (Note that this LET Matrix information supercedes details in *STEREO–CIT–002.F, Appendix 1*, which is out of date as of this version of the LET Science Data Format.)

Particles that are sorted through the matrices are counted in arrays in the LET onboard memory, sorted by penetration range, species (element, charge, charge range, or background), and energy (for elements). Particle counting rates with defined element and energy are termed "foreground rates" (FGRATES), following the curved tracks bounding elements in the Figures in Appendix C. Foreground rates include elements (and helium isotopes) such as H, He-3, He-4, C, N, O, Ne, Na, Mg, Al, Si, Ar, Ca, Fe, and Ni. Particles counted by the FGRATES are assigned Particle IDs which equal their index values in the FGRATES arrays associated with each penetration range (L1L2=L2FGRATES, L2L3=L3FGRATES, L3AL3B=PENFGRATES). These Particle IDs are also used to identify particles in the Event Record Headers, described in Section 2.8. The Particle IDs are given in Tables 3.9–3.14. Particles not located in the FGRATES regions of the matrices, or particles which are otherwise unclassified by the matrices, are assigned a Particle ID of 255. Note that some elements are classified by the Range 3 matrix but not in the other matrices. These particles are also assigned a Particle ID of 255 when located in the Range 2 or Range 4 matrices, e.g. Na in RNG 2 and RNG 4.

Particle IDs may be duplicated between different ranges. While it may be convenient for science analysis for particles having the same charge and energy range in two different matrices to have the same Particle ID, it would add additional load to limited onboard computing resources. It will be less strain on computing resources to account for different Particle IDs during analysis on the ground.

Particles in the matrices which do not fall along element or isotope tracks are termed "background rates" (BGRATES). Background rates are counts from broad regions of delta–E vs E' space in the matrices such as the Li, Be, and B region between He and C, or the "backward moving particles" region to the lower right corner of delta–E vs. E' plots. The background rates also include regions covering STIM events, described elsewhere. All background rate events are assigned Particle ID 255. The background rates are summarized in Tables 3.9–3.14.

Finally, science rate counters are stored in onboard memory in 24 bit counters, but in the Science Frame, these rates are compressed to 16 bits. The format for the compressed, 16 bit rates is shown in Figure 2.1.

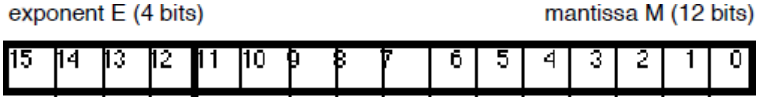

Figure 2.1: 16 bit compressed rate.

The compression algorithm will be a 16 bit modified biased exponent hidden one algorithm, as detailed in Appendix A.

Thus, there are currently 371 Science Rates in the LET Science Data Frame, for a total of 742 bytes.

2.5 Look Direction Rates

Under the current LET Science Frame Format, 8 look directions toward the A side of the LET detector and 8 look directions toward the B side of LET will be counted, for 10 rates in each direction. A total of 160 look direction rates will be encoded in the LET Science Frame. Each look direction rate will be encoded in 16 bit compressed rates, using the same format and compression/decompression algorithm as the science rates. Thus, we send a total of 320 bytes of look direction rates per LET Science Frame.

The look directions are divided into 8 sectors on either side of LET, with detector combinations currently described elsewhere. (See *Options for LET Sectored Rates* and *Final Selection of Sectored Rates (9/29/03)* memos (R.A. Mewaldt).) For the purpose of the LET Science Frame Format, the 8 sectors are numbered 0 through 7, and they are geometrically arranged clockwise around the LET detector, so that sector 0 of LET side A is associated with the L1A0 detector, and sector 7 of LET side A is associated with the L1A4 detector. (See *STEREO/IMPACT LET Detector Naming, STEREO-CIT-0015.B.*) Numbering on the B side begins with direction 8, so that sector 8 of LET side B is associated with the L1B0 detector, and so on.

In addition to look directions, or sectors, these rates are divided into element or element ranges: H, He–3, He-4, CNO, NeMgSi, and Fe. Within each element, these rates are further divided into energy ranges.

Organization of the look direction rates arranged top–down by species, energy range, and look direction, with look direction first on side A (directions 0 through 7) and then side B (directions 8 through 15). The look direction rates are summarized in Section 3, Table 3.15:

2.6 Singles and Coincidence Rates

There are 54 ADCs in LET, and each ADC will be measured for singles rates at low and high gain thresholds. These rates will be compressed to 16 bits, using the same compression/decompression algorithm employed for science and look direction rates. Thus, there will be a total of 108 singles rates in the LET Science Frame, for a total of 216 bytes. The singles rates are given in order of detector address number, which is used by the LET onboard software for detector addressing. The ordering of singles rates in the LET Science Format is top–down by detector number, then by high gain and low gain. Thus, the first four bytes in the Singles Rates block are L2A0 (detector address 0), with the first two bytes being L2A0 high gain singles rate, and the second two bytes being L2A0 low gain singles rate. (Furthermore, given the byte ordering described in Section 2.1, the first byte of the L2A0 high gain singles rate is the high byte, and the second byte is the low byte.) See Section 3, Table 3.4 for a summary of the singles rates and their location in the LET Science Frame, and see the *LET Detector Naming* Document for a description of the detector naming convention.

Coincidence rates are listed in Section 3, Table 3.7. These rates count coincident hits for detector groups for the minute spanned by the Science Frame. Space in the LET Science Frame is allocated for 12 coincidence rates (including 2 unused spares), compressed to 16 bits as with other rates.

2.7 Livetimes, Event Processing Counters, and Priority Buffer Counters

Space is allocated in the LET Science Frame for livetime counters, event processing counters, and priority buffer counters. These counters are event or processing counts used or otherwise maintained by the LET onboard software.

LET Livetimes, event processing counters, and priority buffer counters are listed in Section 3, Tables 3.3, 3.6, and 3.8, respectively. All of the counters are stored as 24 bit numbers in the LET onboard memory, and in the LET Science Format, they are compressed to 16 bits using the same compression algorithm as is used with the science rates. The one exception is the Front End Electronics livetime counter (bytes 8–7 in the LET Science Frame), which is scaled from 24 bits to 16 bits.

Notes on Table 3.3: The NUMTRIG, NUMREJECT, etc. counters are hardware counters, with counters for events taken under hazard (.HAZ) conditions. NUMTRIG is the number of trigger events detected by the hardware during every even numbered second during the minute of accumulation time for the science frame. NUMREJECT is the number of trigger events rejected for further analysis, as determined by hardware conditions described elsewhere. NUMACCPHA is the number of trigger events accepted for further analysis with PHA data, as determined by the hardware. NUMACCNPHA is the number of trigger events accepted for further analysis without PHA data; however, since all accepted events currently include PHA data, this number is always zero.

Under the current definitions, the sum of NUMREJECT and NUMACCPHA should equal NUMTRIG. Because these counters are accumulated only during even numbered seconds, they represent only half the total number of triggers, etc. which could be detected during the entire minute

The equivalent .HAZ counts are those counted under hazard conditions, and these are accumulated during odd numbered seconds during the minute. A trigger event is flagged as a .HAZ event if it comes within 18/6.4 (~2.8) microseconds after the previous trigger. The .HAZ condition is an added condition to the trigger logic; it is not exclusive. Therefore, if NUMTRIG and NUMTRIG.HAZ events were counted simultaneously, the NUMTRIG.HAZ events would count a subset of the NUMTRIG events. The NUMREJECT.HAZ and NUMACCPHA.HAZ events are defined as NUMREJECT and NUMACCPHA events, only with the .HAZ condition added. As with non-.HAZ events, the .HAZ events represent only half the total number of .HAZ events which could occur during a given minute, since they are accumulated only during odd numbered seconds.

Currently, all .HAZ events are rejected for analysis, though this rejection can be commanded on or off. The livetime counter is not incremented during .HAZ events, when such events are rejected for analysis.

2.8 Miscellaneous Bits and Rates

Some information regarding the state of the instrument and software, as well as rates not defined in previous sections, are allocated space in the LET Science Frame. Two bytes of MISCBITS and 10 bytes of MISCRATES are allocated to the LET Science Frame, and these bits and bytes are located in the Frame in Section 3, Tables 3.2 and 3.5. MISCBITS contain information via software flags on the state of the instrument and a minute counter.

2.9 Event Buffer – Event Record Format:

With the fixed format data described in previous sections for the LET Science Frame, there remain 2733 bytes, all of which will be pulse height data in an Event Buffer. Events (pulse heights) are sampled by the LET MISC from priority buffers listed in Section 3, Table 3.8 and the sampled pulse heights are packaged into Event Records in the Event Buffer. The telemetered events will not exceed the Event Buffer length.

At the top of the event buffer will be a header containing the number of events saved to the buffer. If the minimum event length of 2 ADC hits is 72 bits (9 bytes – see below), then the event buffer can contain up to ~303 events, with one 2 byte event buffer header. Unused buffer space will be filled with zeros, and empty packets will not be transmitted.

Within the buffer, each event should be collected in a defined event record, composed of an Event Record Header (ERH) followed by a variable number of ADC fields. The 32 bit Event Record Header is defined as follows:

Table 2.2: Event Record Header (ERH)

Data	Bit	Note
Particle ID	0–7	= particle ID if the particles are sorted by the LET Matrices as "foreground" particles. (=255 if the particles are not sorted by the matrices or are identified as background particles). Allows matrices to ID particles by range (matrix), species, and energy. See Section 3, Tables 3.9–3.14 for lists of Particle IDs. See also *SEP LET and Central MISC Processors Flight Software Requirements* (*STEREO-CIT-CIT-002.F*).
Priority Buffer Number	8–12	See Section 3, Table 3.8 for a list of Priority Buffer Numbers and their descriptions.
L1A Tag	13	Indicates an L1A detector contributed to the coincidence trigger
L2A Tag	14	
L3A Tag	15	
L1B Tag	16	
L2B Tag	17	
L3B Tag	18	
STIM Tag	19	Flags a STIM event.
HAZ Tag	20	Hazard flag.
Time Tag (Latency Bits)	21–24	Duplicates the 4 least significant bits of the LET onboard minutes counter (Section 2.8, and Table 3.2); used to identify event latency
A/B Event Tag	25	A=0, B=1
# Unread ADCs	26–28	# hit ADCs not include in the Event Record. Saturates at 7.
Extended Header Flag	29	=1 if an additional header byte (or set of bytes) is appended to this header
STIM Block Flag	30	=1 if STIM Information Block is included in this event
Culling Flag	31	=1 if number of ADCs culled from this event is nonzero.

The format of the event record header is summarized in Figure 2.2:

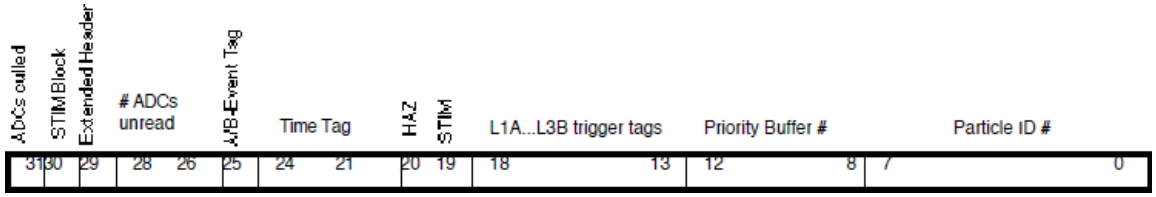

Figure 2.2: Event Record Header, 32 bits.

The particle ID identifies the particle by species and energy, based on how it was sorted through the LET Matrices (Section 3, Tables 3.9–3.14, and Appendix C). If the particle is not a "foreground" event (i.e. if it is not identified as a selected element or helium isotope for a given matrix) and is instead a "background" event, or if the particle is not sorted by the LET matrices, it is assigned a Particle ID of 255. For the identifiable elements targeted by the LET instrument (Table 1.1), the Particle ID is sufficient to identify element and energy.

Additional information is provided by the priority buffer number (bits 8–12). This number identifies the priority buffer from which the Event is taken. Although all events in the Event Buffer are taken from the Priority Buffers, not all events are sorted by the LET Matrices. Not all particles which trigger the LET instrument enter the Priority Buffers. Instead, a sample of trigger events is sent to the Priority Buffers, which are defined and weighted to target particle types according to the goals of the LET instrument. Priority Buffers (listed in Table 3.8) are defined to identify classes of particles by penetration range, by charge or charge range, or by other characteristic (e.g. STIM events). There is some overlap in information between Particle ID and Priority Buffer number. See Section 3, Table 3.8 for a list of Priority Buffer numbers.

The L1A through L3B trigger tags identify which detector groups were involved in the trigger conditions, and the A/B tag identifies which side of the detector provided the trigger. The HAZ flag marks a hazard condition. The STIM flag marks a calibration event defined in *Specification of Functional Test Modules and In-flight Calibration Routines for LET, STEREO-CIT-006.A*. STIM events follow a special format, described in Section 2.10.

The Time Tag (Latency) Bits duplicate the four least significant bits of the minutes field of an onboard clock (LET internal minute counter), as an indicator of event latency. When events are packaged and placed in priority buffers, these minutes bits are copied onto the ERH Latency Bits. Later, when the full Science Frame is packaged into CCSDS packets, the time of the assembly of the Science Frame is copied onto time fields in the CCSDS packet headers and onto the Minutes counter of MISCBITS (Section 2.8, and Table 3.2). Because the time that an event is popped off its priority buffer and placed into the Science Frame may be delayed by more than one minute after the event is first pushed onto the priority buffer, the Latency Bits for a given event may not correspond to the time that the event's Science Frame is assembled. It is up to the user of the data to determine what value of the latency bits precisely corresponds to times associated with given Science Frames. (Note: Previous versions of this document identified the Latency Bits – or Time Tag bits – as counting the age of the event, in minutes, relative to its Science Frame. Also, because the Latency Bits are the 4 least significant bits of a minutes field in a clock, the value of the Latency Bits cycles from 0 to 15 three times, followed by 0 to 11, over the course of an hour.)

For some classes of events, large numbers of detectors or ADCs in the LET instrument may be triggered and result in signals. The LET Data Format (Event Record Format) described herein is capable of returning events with the maximum of 54 ADC hits. Most of these events are unlikely to be sorted by the LET Matrices, but some fraction of them will be sent to the Event Buffer. For events with sufficiently large numbers of hit ADCs, not all ADCs will be included in the Event Record. The onboard software will determine the maximum number of ADC signals transmitted for each event. Bits 25–27 will count the number of ADCs in the event which are **not** included in the Event Record, with a saturation value of 7.

A separate number counting the ADCs **included** in the Event Record is not included in the Event Record Header. Instead, and End of Record (EOR) bit is employed in the ADC Field, described later in this section. Furthermore, LET has a VERBOSE mode in which both low gain and high gain signals from a given ADC may be transmitted. By relying on the EOR bit in the ADC Fields, the format allows for transmission of low and high gain signals for any given ADC, and the EOR bit itself is sufficient to mark the length of an Event Record.

An Extended Header flag (bit 29) marks the addition 2 bytes of header information, described in Section 2.11. A STIM block flag (bit 30) marks the addition 2 bytes of STIM block information to the header, described in Section 2.10. A final ADC culling flag (bit 31) marks the condition that one or more ADCs were culled by onboard software for the event. If culling mode is off, this bit is always zero.

Following the header are a number of ADC fields. Each ADC field will contain the following:

Table 2.3: ADC Field — Minimum Bit Allocations

Data	**# Bits**	**Note**
ADC Signal	12	11 bits signal, 1 bit overflow
ADC/Detector ID	6	54 detectors maximum
Low/High gain	1	0 = low gain, 1 = high gain
Last hit flag (End of Record, EOR)	1	Set to 1 for the last ADC in an event, 0 for all other ADCs

Thus, each ADC signal and identifier is encoded in 20 bits. Note that the End of Record (EOR) bit is 0 except when set to 1 for the last ADC Field in an event record. The detector ID is the same as the detector address, a list of which can be found with the singles rates table, Section 3, Table 3.4. The format of the ADC Field is given in Figure 2.3:

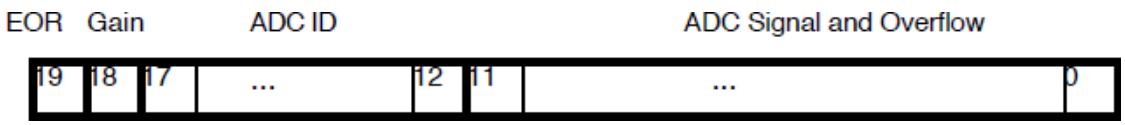

Figure 2.3: Event Record ADC Field. End of Record (EOR) and Gain bits are defined in Table 2.3.

The smallest event record (one event record header plus 2 ADC Fields) would be 72 bits long. A 3 ADC event would be 92 bits long. The event records will be padded by 4 bits for each event record with odd numbers of ADC Fields, allowing all event records to be aligned to byte boundaries. Table 2.4 and Figures 2.4–2.5 show some examples, with the Figures diagramming Event Records as 3 bytes wide for illustration only.

Table 2.4: Bit padding of Event Records.

# ADC Fields	# bits without padding	Padding bits	# bytes with padding
2	72	0	9
3	92	4	12
4	112	0	14
5	132	4	17
6	152	0	19
7	172	4	22

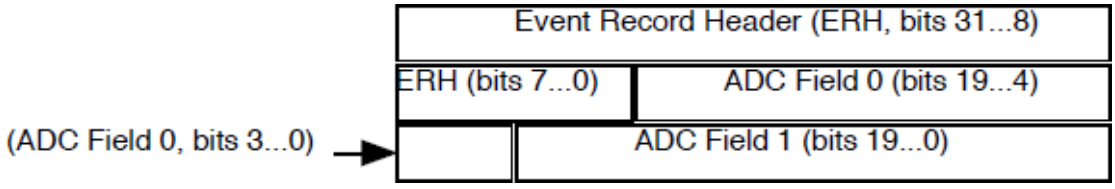

Figure 2.4: Event Record with 2 ADC Fields. Left to right is MSB to LSB, spanning 3 bytes.

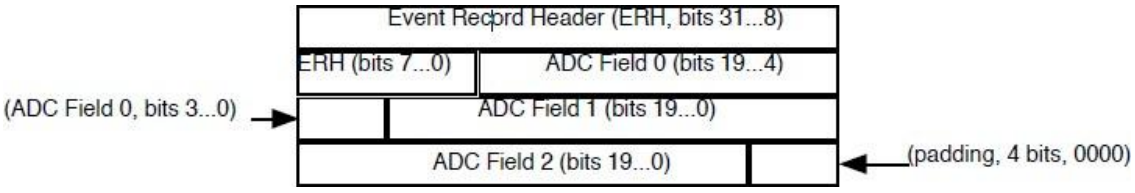

Figure 2.5: Event Record with 3 ADC Fields. Left to right is MSB to LSB, spanning 3 bytes.

Note: In the event of a bit error, particularly in the End of Record (EOR) bit in the ADC field, it is possible that all subsequent events in the Event Buffer will be unreconstructible or, at the very least, very difficult to reconstruct. Such bit errors are expected to be extremely rare. Possible remedies in the Event Record format may include enforcing MISC word boundaries for the ADC Field, and forcing bit 23 (EOR bit) in such ADC Fields to be 0 except at EOR. The disadvantage of this approach is an increase in the length in bytes of some events. The increasing number of unused bits in each event record will reduce the number of events possible in an Event Buffer.

Given the sizes of the Event Records and the included 4 bit padding of odd-number ADC events, Table 2.5 summarizes the Event Buffer capacity and the Telemetry Rate for events of up to 7 ADCs:

Table 2.5: Event Buffer Capacity and Telemetry Rate

# ADCs	Maximum # Events in Buffer	Telemetry Rate (events/sec)
2	303	5.1
3	227	3.8
4	195	3.3
5	160	2.7
6	143	2.4
7	124	2.1

Note that these estimates assume that the STIM Information Block (Section 2.10) and the Extended Header Block (Section 2.11) are not included in the event record.

2.10 Event Buffer – STIM Events

Bit 19 of the Event Record Header flags calibration, or STIM, events. These events include livetime STIM events and ADC STIM events. Both of these types of STIM events will be included in the Event Buffer, with different priorities and different (or unassigned) particle IDs. However, because they represent a different class of event than regular particles, it is anticipated that additional information may be needed for calibration and identification. Therefore, an additional 3-byte STIM Information Block is appended to the Event Record for STIM events, after the ADC fields and optional Extended Header block.

A two ADC STIM event is shown in Figure 2.6.

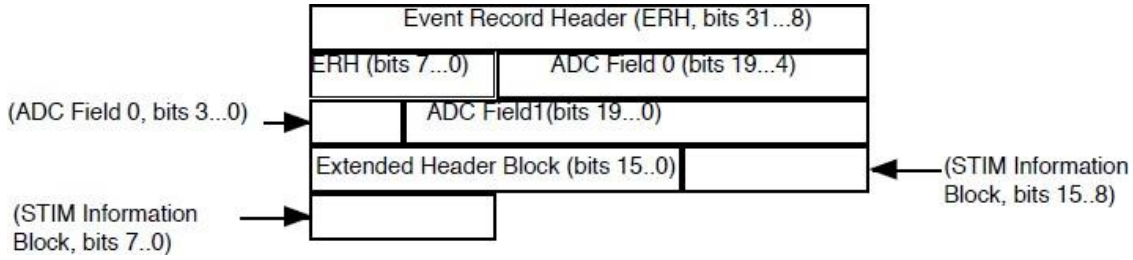

Figure 2.6: Event Record with 2 ADC Fields. Left to right is MSB to LSB, spanning 3 bytes. Optional Extended Header Block is also attached.

STIM events will be padded to fill out bytes in the same way that regular events are padded, at the end of the event record.

The STIM Information Block is appended after the Event Record Header if bit 30 of the ERH is set. The STIM information block contains a "seconds" counter, the DACLEVEL, and the DACCONFIGURATION. The seconds counter contains the second number within the accumulation minute of the LET Science Frame during which the STIM event was taken. For example, during normal mode operation, livetime STIM events are accumulated during the 0-8 second, 10-18 second, 20-28 second, etc. time intervals, while ADC STIM events are accumulated at the 9 second, 19 second, 29 second, etc. points. The DACLEVEL (0-31) and DACCONFIGURATION (0-14) indicate via tables in the LET onboard software what the DAC settings are for the STIM events and which ADCs are stimulated, respectively.

The bit assignments are defined elsewhere. The assumed arrangement of bits is shown in Figure 2.7.

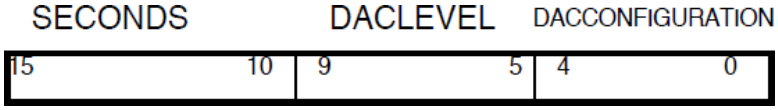

Figure 2.7: STIM Information Block

2.11 Extended Header Block

If bit 29 of the Event Record Header is set, an additional two byte Extended Header Block (or Extended Information Block) is appended after the ERH and ADC fields and before an optional STIM Information Block (Section 2.10). This Extended Header Block contains additional information useful for diagnosing onboard software function and performance.

The Extended Header Block currently contains DEINDEX (9 bits) and EPINDEX (7 bits). DEINDEX is the delta-E axis matrix index generated by the onboard software to map the given event to a LET Matrix Map (see Appendix C). It has a value in the range 0-399. EPINDEX is the residual energy axis matrix index (E-prime) generated by the onboard software to map the given event to a LET Matrix Map, and it has a value in the range 0-127.

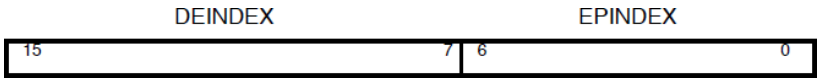

Figure 2.8: Extended Header Block

3.0 LET Science Frame Format Summary

Tables 3.1–3.16 summarize the LET Science Data Frame Format, viewing the LET Data Frame as a stream of numbered bytes (0-4159). Descriptions of the contents of the Science Frame are given in Section 2, but these tables provide the byte locations of data elements in the LET Science Frame.

Note that the Science/Foreground Rates tables are quite long and span multiple pages.

Table 3.1: LET Science Data Frame Header Summary

Frame Byte # (First)	Frame Byte # (Last)	Description
0	0	Bits 6-7 = 00 (EM unit), 01 (FM1, ahead), 10 (FM2, behind) Bits 0-5 = frame version number
1	2	# Bytes used in Frame (SFLEN)
3	4	LET Science Frame Checksum (SFCHECK)

Table 3.2: Miscellaneous Bits, MISCBITS

Frame Byte # (First)	Frame Byte # (Last)	Description
5	5	Bit 7 = CodeOK Bits 3-6 = HeaterDutyCycle Bit 2 = LeakConv Bits 0-1 = DyThState
6	6	Minute (LET internal minute counter)

Table 3.3: Livetime Counters, ERATES

Frame Byte # (First)	Frame Byte # (Last)	Description
7	8	Livetime counter, Front End Electronics
9	10	# Triggers (NUMTRIG)
11	12	# Rejected Events (NUMREJECT)
13	14	# Accepted Events with PHA data (NUMACCPHA)
15	16	# Accepted Events without PHA data (NUMACCNPHA)
17	18	NUMTRIG.HAZ
19	20	NUMREJECT.HAZ
21	22	NUMACCPHA.HAZ
23	24	NUMACCNPHA.HAZ

Table 3.4: Singles Rates, SNGRATES

Frame Byte # (First)	Frame Byte # (Last)	# Bytes	Description	Detector Address
25	28	4	L2A0, High and Low Gain	0
29	32	4	L2A1, High and Low Gain	1
33	36	4	L2A2, High and Low Gain	2
37	40	4	L2A3, High and Low Gain	3
41	44	4	L2A4, High and Low Gain	4
45	48	4	L2A5, High and Low Gain	5
49	52	4	L2A6, High and Low Gain	6
53	56	4	L2A7, High and Low Gain	7
57	60	4	L2A8, High and Low Gain	8
61	64	4	L2A9, High and Low Gain	9
65	68	4	L3Ai, High and Low Gain	14
69	72	4	L3Ao, High and Low Gain	15
73	76	4	L1A0a, High and Low Gain	16
77	80	4	L1A0b, High and Low Gain	17
81	84	4	L1A0c, High and Low Gain	18
85	88	4	L1A1a, High and Low Gain	19
89	92	4	L1A1b, High and Low Gain	20
93	96	4	L1A1c, High and Low Gain	21
97	100	4	L1A2a, High and Low Gain	22
101	104	4	L1A2b, High and Low Gain	23
105	108	4	L1A2c, High and Low Gain	24
109	112	4	L1A3a, High and Low Gain	25
113	116	4	L1A3b, High and Low Gain	26
117	120	4	L1A3c, High and Low Gain	27
121	124	4	L1A4a, High and Low Gain	28
125	128	4	L1A4b, High and Low Gain	29
129	132	4	L1A4c, High and Low Gain	30
133	136	4	L1B0a, High and Low Gain	32
137	140	4	L1B0b, High and Low Gain	33
141	144	4	L1B0c, High and Low Gain	34
145	148	4	L1B1a, High and Low Gain	35
149	152	4	L1B1b, High and Low Gain	36
153	156	4	L1B1c, High and Low Gain	37
157	160	4	L1B2a, High and Low Gain	38
161	164	4	L1B2b, High and Low Gain	39
165	168	4	L1B2c, High and Low Gain	40
169	172	4	L1B3a, High and Low Gain	41

173	176	4	L1B3b, High and Low Gain	42
177	180	4	L1B3c, High and Low Gain	43
181	184	4	L1B4a, High and Low Gain	44
185	188	4	L1B4b, High and Low Gain	45
189	192	4	L1B4c, High and Low Gain	46
193	196	4	L2B0, High and Low Gain	48
197	200	4	L2B1, High and Low Gain	49
201	204	4	L2B2, High and Low Gain	50
205	208	4	L2B3, High and Low Gain	51
209	212	4	L2B4, High and Low Gain	52
213	216	4	L2B5, High and Low Gain	53
217	220	4	L2B6, High and Low Gain	54
221	224	4	L2B7, High and Low Gain	55
225	228	4	L2B8, High and Low Gain	56
229	232	4	L2B9, High and Low Gain	57
233	236	4	L3Bi, High and Low Gain	62
237	240	4	L3Bo, High and Low Gain	63

Table 3.5: Miscellaneous Rates, MISCRATES (**unused**)

Frame Byte # (First)	**Frame Byte # (Last)**	**# Bytes**	**Description**
241	250	10	Miscellaneous instrument rates (unused)

Table 3.6: Event Processing Rates, EVPRATES

Frame Byte # (First)	**Frame Byte # (Last)**	**Description**
251	252	NREAD (events read from event FIFO)
253	254	NHAZ (events rejected for Hazard condition)
255	256	NADCSTIM (ADC-calibration STIM events)
257	258	NODD (odd events)
259	260	NODDFIX (fixed odd events)
261	262	NMULTI (events with multiple hits in relevant layers)
263	264	NMULTIFIX (fixed multi events)
265	266	NBADTRAJ (events rejected for inconsistent/bad trajectory)
267	268	NL2 (events sorted into L12 event category)
269	270	NL3 (events sorted into L123 event category)
271	272	NPEN (events sorted into PEN event category)
273	274	NFORMAT (events handled by the telemetry event formatter)
275	276	NASIDE (events the software assumed were Aside events)
277	278	NBSIDE (events the software assumed were Bside events)
279	280	NERROR (events that caused a processing error - should never happen)
281	282	NBADTAGS (events with bad tags from onboard event-processing)

Table 3.7: Coincidence Rates, COINRATES

Frame Byte # (First)	Frame Byte # (Last)	# Bytes	Description
283	284	2	L12A
285	286	2	L123A
287	288	2	PENA
289	290	2	spare
291	292	2	L12B
293	294	2	L123B
295	296	2	PENB
297	298	2	spare
299	300	2	PENA?
301	302	2	PENB?
303	304	2	2TEL
305	306	2	ERRTAG

Table 3.8: Priority Buffer Rates, BUFRATES

Frame Byte # (First)	Frame Byte # (Last)	Description
307	308	PB #0 ADC-cal events
309	310	PB #1 Range 2, 3, or 4 events that fall into Z>=40 matrix box
311	312	PB #2 Range 2, 3, or 4 events that fall into 31<=Z<=39 matrix box
313	314	PB #3 Range 3 events that fall into 9<=Z<=30 matrix box, or any foreground box that is painted over it.
315	316	PB #4 Range 2 events that fall into 9<=Z<=30 matrix box, or any foreground box that is painted over it.
317	318	PB #5 Range 3 events that fall into the LiBeB, CNO, C, N, or O matrix boxes
319	320	PB #6 Range 2 events that fall into the LiBeB, CNO, C, N, or O matrix boxes
321	322	PB #7 Range 4 events that fall into the LiBeB, CNO, or 9<=Z<=30 matrix boxes, or any foreground matrix box from C thru Ni.
323	324	PB #8 Range 4 events that fall into the PEN_Z>30 matrix box ("penetrating" or "Range 5" events)
325	326	PB #9 Matrix-sort Reject events, with L3 signal, Z>=3
327	328	PB #10 Matrix-sort Reject events, with NO L3 signal, Z>=3
329	330	PB #11 Range 3 events that fall into 3He matrix box
331	332	PB #12 Range 2 events that fall into 3He matrix box
333	334	PB #13 Range 4 events that fall into the PEN_3<=Z<=30 matrix box ("penetrating" or "Range 5" events)
335	336	PB #14 Range 3 events that fall into the He background or 4He foreground matrix box
337	338	PB #15 Range 4 events that fall into any He matrix box
339	340	PB #16 Range 2 events that fall into the He background or 4He foreground matrix box
341	342	PB #17 Range 3 events that fall into any H matrix box
343	344	PB #18 Range 4 events that fall into any H matrix box
345	346	PB #19 Range 2 events that fall into any H matrix box
347	348	PB #20 Matrix-sort Reject events, with L3 signal, Z<3
349	350	PB #21 Matrix-sort Reject events, with NO L3 signal, Z<3

351	352	PB #22 Range 4 events that fall into the PEN_H_He matrix box ("penetrating" or "Range 5" events)
353	354	PB #23 Range 2, 3, or 4 events that fall into the "Backward" matrix box
355	356	PB #24 "Clean" Livetime STIM events (stim events that fall into a STIM matrix box)
357	358	PB #25 "Poor" Livetime STIM events (stim events that either fall outside a STIM matrix box, or are rejected because of multiple hits in a layer, etc.)
359	360	PB #26 ERROR - Onboard processing of the event was aborted due to an error. Occurs if the tag-bits of the event are invalid. Can also occur if the onboard processing reaches a point that it should never reach.
361	362	PB #27 Other - currently not used
363	364	PB #28 Spare

Table 3.9: LET Science Data Frame, Range 2 (L1L2) Science/Foreground Rates, L2FGRATES

Frame Byte # (First)	Frame Byte # (Last)	Description	Particle ID
365	366	H (1.0-1.8 MeV/nuc)	0
367	368	H (1.8-2.2 MeV/nuc)	1
369	370	H (2.2-2.7 MeV/nuc)	2
371	372	H (2.7-3.2 MeV/nuc)	3
373	374	H (3.2-3.6 MeV/nuc)	4
375	376	H (3.6-4.0 MeV/nuc)	5
377	378	H (4.0-4.5 MeV/nuc)	6
379	380	H (4.5-5.0 MeV/nuc)	7
381	382	H (5.0-70.0 MeV/nuc)	8
383	384	He-3 (1.0-2.2 MeV/nuc)	9
385	386	He-3 (2.2-2.7 MeV/nuc)	10
387	388	He-3 (2.7-3.2 MeV/nuc)	11
389	390	He-3 (3.2-3.6 MeV/nuc)	12
391	392	He-3 (3.6-4.0 MeV/nuc)	13
393	394	He-3 (4.0-4.5 MeV/nuc)	14
395	396	He-3 (4.5-5.0 MeV/nuc)	15
397	398	He-3 (5.0-6.0 MeV/nuc)	16
399	400	He-3 (6.0-70.0 MeV/nuc)	17
401	402	He-4 (1.0-1.8 MeV/nuc)	18
403	404	He-4 (1.8-2.2 MeV/nuc)	19
405	406	He-4 (2.2-2.7 MeV/nuc)	20
407	408	He-4 (2.7-3.2 MeV/nuc)	21
409	410	He-4 (3.2-3.6 MeV/nuc)	22
411	412	He-4 (3.6-4.0 MeV/nuc)	23
413	414	He-4 (4.0-4.5 MeV/nuc)	24
415	416	He-4 (4.5-5.0 MeV/nuc)	25
417	418	He-4 (5.0-70.0 MeV/nuc)	26
419	420	C (1.0-3.2 MeV/nuc)	27
421	422	C (3.2-3.6 MeV/nuc)	28
423	424	C (3.6-4.0 MeV/nuc)	29
425	426	C (4.0-4.5 MeV/nuc)	30
427	428	C (4.5-5.0 MeV/nuc)	31
429	430	C (5.0-6.0 MeV/nuc)	32

431	432	C (6.0-8.0 MeV/nuc)	33
433	434	C (8.0-10.0 MeV/nuc)	34
435	436	C (10.0-70.0 MeV/nuc)	35
437	438	N (1.0-3.2 MeV/nuc)	36
439	440	N (3.2-3.6 MeV/nuc)	37
441	442	N (3.6-4.0 MeV/nuc)	38
443	444	N (4.0-4.5 MeV/nuc)	39
445	446	N (4.5-5.0 MeV/nuc)	40
447	448	N (5.0-6.0 MeV/nuc)	41
449	450	N (6.0-8.0 MeV/nuc)	42
451	452	N (8.0-10.0 MeV/nuc)	43
453	454	N (10.0-70.0 MeV/nuc)	44
455	456	O (1.0-3.2 MeV/nuc)	45
457	458	O (3.2-3.6 MeV/nuc)	46
459	460	O (3.6-4.0 MeV/nuc)	47
461	462	O (4.0-4.5 MeV/nuc)	48
463	464	O (4.5-5.0 MeV/nuc)	49
465	466	O (5.0-6.0 MeV/nuc)	50
467	468	O (6.0-8.0 MeV/nuc)	51
469	470	O (8.0-10.0 MeV/nuc)	52
471	472	O (10.0-70.0 MeV/nuc)	53
473	474	Ne (1.0-3.2 MeV/nuc)	54
475	476	Ne (3.2-3.6 MeV/nuc)	55
477	478	Ne (3.6-4.0 MeV/nuc)	56
479	480	Ne (4.0-4.5 MeV/nuc)	57
481	482	Ne (4.5-5.0 MeV/nuc)	58
483	484	Ne (5.0-6.0 MeV/nuc)	59
485	486	Ne (6.0-8.0 MeV/nuc)	60
487	488	Ne (8.0-10.0 MeV/nuc)	61
489	490	Ne (10.0-12.0 MeV/nuc)	62
491	492	Ne (12.0-70.0 MeV/nuc)	63
493	494	Mg (1.0-3.2 MeV/nuc)	64
495	496	Mg (3.2-3.6 MeV/nuc)	65
497	498	Mg (3.6-4.0 MeV/nuc)	66
499	500	Mg (4.0-4.5 MeV/nuc)	67
501	502	Mg (4.5-5.0 MeV/nuc)	68
503	504	Mg (5.0-6.0 MeV/nuc)	69
505	506	Mg (6.0-8.0 MeV/nuc)	70
507	508	Mg (8.0-10.0 MeV/nuc)	71
509	510	Mg (10.0-12.0 MeV/nuc)	72
511	512	Mg (12.0-15.0 MeV/nuc)	73
513	514	Mg (15.0-70.0 MeV/nuc)	74
515	516	Si (1.0-3.2 MeV/nuc)	75
517	518	Si (3.2-3.6 MeV/nuc)	76
519	520	Si (3.6-4.0 MeV/nuc)	77
521	522	Si (4.0-4.5 MeV/nuc)	78
523	524	Si (4.5-5.0 MeV/nuc)	79
525	526	Si (5.0-6.0 MeV/nuc)	80
527	528	Si (6.0-8.0 MeV/nuc)	81
529	530	Si (8.0-10.0 MeV/nuc)	82
531	532	Si (10.0-12.0 MeV/nuc)	83
533	534	Si (12.0-15.0 MeV/nuc)	84

535	536	Si (15.0-70.0 MeV/nuc)	85
537	538	S (1.0-3.6 MeV/nuc)	86
539	540	S (3.6-4.0 MeV/nuc)	87
541	542	S (4.0-4.5 MeV/nuc)	88
543	544	S (4.5-5.0 MeV/nuc)	89
545	546	S (5.0-6.0 MeV/nuc)	90
547	548	S (6.0-8.0 MeV/nuc)	91
549	550	S (8.0-10.0 MeV/nuc)	92
551	552	S (10.0-12.0 MeV/nuc)	93
553	554	S (12.0-15.0 MeV/nuc)	94
555	556	S (15.0-70.0 MeV/nuc)	95
557	558	Ar (1.0-3.6 MeV/nuc)	96
559	560	Ar (3.6-4.0 MeV/nuc)	97
561	562	Ar (4.0-4.5 MeV/nuc)	98
563	564	Ar (4.5-5.0 MeV/nuc)	99
565	566	Ar (5.0-6.0 MeV/nuc)	100
567	568	Ar (6.0-8.0 MeV/nuc)	101
569	570	Ar (8.0-10.0 MeV/nuc)	102
571	572	Ar (10.0-12.0 MeV/nuc)	103
573	574	Ar (12.0-15.0 MeV/nuc)	104
575	576	Ar (15.0-21.0 MeV/nuc)	105
577	578	Ar (21.0-70.0 MeV/nuc)	106
579	580	Ca (1.0-3.6 MeV/nuc)	107
581	582	Ca (3.6-4.0 MeV/nuc)	108
583	584	Ca (4.0-4.5 MeV/nuc)	109
585	586	Ca (4.5-5.0 MeV/nuc)	110
587	588	Ca (5.0-6.0 MeV/nuc)	111
589	590	Ca (6.0-8.0 MeV/nuc)	112
591	592	Ca (8.0-10.0 MeV/nuc)	113
593	594	Ca (10.0-12.0 MeV/nuc)	114
595	596	Ca (12.0-15.0 MeV/nuc)	115
597	598	Ca (15.0-21.0 MeV/nuc)	116
599	600	Ca (21.0-70.0 MeV/nuc)	117
601	602	Fe (1.0-2.7 MeV/nuc)	118
603	604	Fe (2.7-3.2 MeV/nuc)	119
605	606	Fe (3.2-3.6 MeV/nuc)	120
607	608	Fe (3.6-4.0 MeV/nuc)	121
609	610	Fe (4.0-4.5 MeV/nuc)	122
611	612	Fe (4.5-5.0 MeV/nuc)	123
613	614	Fe (5.0-6.0 MeV/nuc)	124
615	616	Fe (6.0-8.0 MeV/nuc)	125
617	618	Fe (8.0-10.0 MeV/nuc)	126
619	620	Fe (10.0-12.0 MeV/nuc)	127
621	622	Fe (12.0-15.0 MeV/nuc)	128
623	624	Fe (15.0-21.0 MeV/nuc)	129
625	626	Fe (21.0-70.0 MeV/nuc)	130
627	628	Na, Al, Ni, unidentified	255

Table 3.10: LET Science Data Frame, Range 2 (L1L2) Science/Background Rates, L2BGRATES

Frame Byte # (First)	Frame Byte # (Last)	Description	Particle ID
629	630	H Background	255
631	632	He Background	255
633	634	LiBeB Background	255
635	636	CNO Background	255
637	638	Z=9-30 Background	255
639	640	Z=30-40 Background	255
641	642	Z>=40 Background	255
643	644	Backward Background	255
645	646	H, He STIM	255
647	648	CNO STIM	255
649	650	Fe STIM	255
651	652	STIM error	255

Table 3.11: LET Science Data Frame, Range 3 (L2L3) Science/Foreground Rates, L3FGRATES

Frame Byte # (First)	Frame Byte # (Last)	Description	Particle ID
653	654	H (1.0-3.2 MeV/nuc)	0
655	656	H (3.2-3.6 MeV/nuc)	1
657	658	H (3.6-4.0 MeV/nuc)	2
659	660	H (4.0-4.5 MeV/nuc)	3
661	662	H (4.5-5.0 MeV/nuc)	4
663	664	H (5.0-6.0 MeV/nuc)	5
665	666	H (6.0-8.0 MeV/nuc)	6
667	668	H (8.0-10.0 MeV/nuc)	7
669	670	H (10.0-12.0 MeV/nuc)	8
671	672	H (12.0-15.0 MeV/nuc)	9
673	674	H (15.0-70.0 MeV/nuc)	10
675	676	He-3 (1.0-4.0 MeV/nuc)	11
677	678	He-3 (4.0-4.5 MeV/nuc)	12
679	680	He-3 (4.5-5.0 MeV/nuc)	13
681	682	He-3 (5.0-6.0 MeV/nuc)	14
683	684	He-3 (6.0-8.0 MeV/nuc)	15
685	686	He-3 (8.0-10.0 MeV/nuc)	16
687	688	He-3 (10.0-12.0 MeV/nuc)	17
689	690	He-3 (12.0-15.0 MeV/nuc)	18
691	692	He-3 (15.0-70.0 MeV/nuc)	19
693	694	He-4 (1.0-3.2 MeV/nuc)	20
695	696	He-4 (3.2-3.6 MeV/nuc)	21
697	698	He-4 (3.6-4.0 MeV/nuc)	22
699	700	He-4 (4.0-4.5 MeV/nuc)	23
701	702	He-4 (4.5-5.0 MeV/nuc)	24
703	704	He-4 (5.0-6.0 MeV/nuc)	25
705	706	He-4 (6.0-8.0 MeV/nuc)	26
707	708	He-4 (8.0-10.0 MeV/nuc)	27
709	710	He-4 (10.0-12.0 MeV/nuc)	28
711	712	He-4 (12.0-15.0 MeV/nuc)	29
713	714	He-4 (15.0-70.0 MeV/nuc)	30
715	716	C (1.0-4.5 MeV/nuc)	31

717	718	C (4.5-5.0 MeV/nuc)	32
719	720	C (5.0-6.0 MeV/nuc)	33
721	722	C (6.0-8.0 MeV/nuc)	34
723	724	C (8.0-10.0 MeV/nuc)	35
725	726	C (10.0-12.0 MeV/nuc)	36
727	728	C (12.0-15.0 MeV/nuc)	37
729	730	C (15.0-21.0 MeV/nuc)	38
731	732	C (21.0-27.0 MeV/nuc)	39
733	734	C (27.0-33.0 MeV/nuc)	40
735	736	C (33.0-70.0 MeV/nuc)	41
737	738	N (1.0-5.0 MeV/nuc)	42
739	740	N (5.0-6.0 MeV/nuc)	43
741	742	N (6.0-8.0 MeV/nuc)	44
743	744	N (8.0-10.0 MeV/nuc)	45
745	746	N (10.0-12.0 MeV/nuc)	46
747	748	N (12.0-15.0 MeV/nuc)	47
749	750	N (15.0-21.0 MeV/nuc)	48
751	752	N (21.0-27.0 MeV/nuc)	49
753	754	N (27.0-33.0 MeV/nuc)	50
755	756	N (33.0-70.0 MeV/nuc)	51
757	758	O (1.0-5.0 MeV/nuc)	52
759	760	O (5.0-6.0 MeV/nuc)	53
761	762	O (6.0-8.0 MeV/nuc)	54
763	764	O (8.0-10.0 MeV/nuc)	55
765	766	O (10.0-12.0 MeV/nuc)	56
767	768	O (12.0-15.0 MeV/nuc)	57
769	770	O (15.0-21.0 MeV/nuc)	58
771	772	O (21.0-27.0 MeV/nuc)	59
773	774	O (27.0-33.0 MeV/nuc)	60
775	776	O (33.0-70.0 MeV/nuc)	61
777	778	Ne (1.0-6.0 MeV/nuc)	62
779	780	Ne (6.0-8.0 MeV/nuc)	63
781	782	Ne (8.0-10.0 MeV/nuc)	64
783	784	Ne (10.0-12.0 MeV/nuc)	65
785	786	Ne (12.0-15.0 MeV/nuc)	66
787	788	Ne (15.0-21.0 MeV/nuc)	67
789	790	Ne (21.0-27.0 MeV/nuc)	68
791	792	Ne (27.0-33.0 MeV/nuc)	69
793	794	Ne (33.0-40.0 MeV/nuc)	70
795	796	Ne (40.0-70.0 MeV/nuc)	71
797	798	Na (1.0-6.0 MeV/nuc)	72
799	800	Na (6.0-8.0 MeV/nuc)	73
801	802	Na (8.0-10.0 MeV/nuc)	74
803	804	Na (10.0-12.0 MeV/nuc)	75
805	806	Na (12.0-15.0 MeV/nuc)	76
807	808	Na (15.0-21.0 MeV/nuc)	77
809	810	Na (21.0-27.0 MeV/nuc)	78
811	812	Na (27.0-33.0 MeV/nuc)	79
813	814	Na (33.0-40.0 MeV/nuc)	80
815	816	Na (40.0-70.0 MeV/nuc)	81
817	818	Mg (1.0-6.0 MeV/nuc)	82
819	820	Mg (6.0-8.0 MeV/nuc)	83

821	822	Mg (8.0-10.0 MeV/nuc)	84
823	824	Mg (10.0-12.0 MeV/nuc)	85
825	826	Mg (12.0-15.0 MeV/nuc)	86
827	828	Mg (15.0-21.0 MeV/nuc)	87
829	830	Mg (21.0-27.0 MeV/nuc)	88
831	832	Mg (27.0-33.0 MeV/nuc)	89
833	834	Mg (33.0-40.0 MeV/nuc)	90
835	836	Mg (40.0-52.0 MeV/nuc)	91
837	838	Mg (52.0-70.0 MeV/nuc)	92
839	840	Al (1.0-6.0 MeV/nuc)	93
841	842	Al (6.0-8.0 MeV/nuc)	94
843	844	Al (8.0-10.0 MeV/nuc)	95
845	846	Al (10.0-12.0 MeV/nuc)	96
847	848	Al (12.0-15.0 MeV/nuc)	97
849	850	Al (15.0-21.0 MeV/nuc)	98
851	852	Al (21.0-27.0 MeV/nuc)	99
853	854	Al (27.0-33.0 MeV/nuc)	100
855	856	Al (33.0-40.0 MeV/nuc)	101
857	858	Al (40.0-52.0 MeV/nuc)	102
859	860	Al (52.0-70.0 MeV/nuc)	103
861	862	Si (1.0-6.0 MeV/nuc)	104
863	864	Si (6.0-8.0 MeV/nuc)	105
865	866	Si (8.0-10.0 MeV/nuc)	106
867	868	Si (10.0-12.0 MeV/nuc)	107
869	870	Si (12.0-15.0 MeV/nuc)	108
871	872	Si (15.0-21.0 MeV/nuc)	109
873	874	Si (21.0-27.0 MeV/nuc)	110
875	876	Si (27.0-33.0 MeV/nuc)	111
877	878	Si (33.0-40.0 MeV/nuc)	112
879	880	Si (40.0-52.0 MeV/nuc)	113
881	882	Si (52.0-70.0 MeV/nuc)	114
883	884	S (1.0-6.0 MeV/nuc)	115
885	886	S (6.0-8.0 MeV/nuc)	116
887	888	S (8.0-10.0 MeV/nuc)	117
889	890	S (10.0-12.0 MeV/nuc)	118
891	892	S (12.0-15.0 MeV/nuc)	119
893	894	S (15.0-21.0 MeV/nuc)	120
895	896	S (21.0-27.0 MeV/nuc)	121
897	898	S (27.0-33.0 MeV/nuc)	122
899	900	S (33.0-40.0 MeV/nuc)	123
901	902	S (40.0-52.0 MeV/nuc)	124
903	904	S (52.0-70.0 MeV/nuc)	125
905	906	Ar (1.0-6.0 MeV/nuc)	126
907	908	Ar (6.0-8.0 MeV/nuc)	127
909	910	Ar (8.0-10.0 MeV/nuc)	128
911	912	Ar (10.0-12.0 MeV/nuc)	129
913	914	Ar (12.0-15.0 MeV/nuc)	130
915	916	Ar (15.0-21.0 MeV/nuc)	131
917	918	Ar (21.0-27.0 MeV/nuc)	132
919	920	Ar (27.0-33.0 MeV/nuc)	133
921	922	Ar (33.0-40.0 MeV/nuc)	134
923	924	Ar (40.0-52.0 MeV/nuc)	135

925	926	Ar (52.0-70.0 MeV/nuc)	136
927	928	Ca (1.0-8.0 MeV/nuc)	137
929	930	Ca (8.0-10.0 MeV/nuc)	138
931	932	Ca (10.0-12.0 MeV/nuc)	139
933	934	Ca (12.0-15.0 MeV/nuc)	140
935	936	Ca (15.0-21.0 MeV/nuc)	141
937	938	Ca (21.0-27.0 MeV/nuc)	142
939	940	Ca (27.0-33.0 MeV/nuc)	143
941	942	Ca (33.0-40.0 MeV/nuc)	144
943	944	Ca (40.0-52.0 MeV/nuc)	145
945	946	Ca (52.0-70.0 MeV/nuc)	146
947	948	Fe (1.0-8.0 MeV/nuc)	147
949	950	Fe (8.0-10.0 MeV/nuc)	148
951	952	Fe (10.0-12.0 MeV/nuc)	149
953	954	Fe (12.0-15.0 MeV/nuc)	150
955	956	Fe (15.0-21.0 MeV/nuc)	151
957	958	Fe (21.0-27.0 MeV/nuc)	152
959	960	Fe (27.0-33.0 MeV/nuc)	153
961	962	Fe (33.0-40.0 MeV/nuc)	154
963	964	Fe (40.0-52.0 MeV/nuc)	155
965	966	Fe (52.0-70.0 MeV/nuc)	156
967	968	Ni (1.0-8.0 MeV/nuc)	157
969	970	Ni (8.0-10.0 MeV/nuc)	158
971	972	Ni (10.0-12.0 MeV/nuc)	159
973	974	Ni (12.0-15.0 MeV/nuc)	160
975	976	Ni (15.0-21.0 MeV/nuc)	161
977	978	Ni (21.0-27.0 MeV/nuc)	162
979	980	Ni (27.0-33.0 MeV/nuc)	163
981	982	Ni (33.0-40.0 MeV/nuc)	164
983	984	Ni (40.0-52.0 MeV/nuc)	165
985	986	Ni (52.0-70.0 MeV/nuc)	166

Table 3.12: LET Science Data Frame, Range 3 (L2L3) Science/Background Rates, L3BGRATES

Frame Byte # (First)	Frame Byte # (Last)	Description	Particle ID
987	988	H Background	255
989	990	He Background	255
991	992	LiBeB Background	255
993	994	CNO Background	255
995	996	Z=9-30 Background	255
997	998	Z=30-40 Background	255
999	1000	Z>=40 Background	255
1001	1002	Backward Background	255
1003	1004	H, He STIM	255
1005	1006	CNO STIM	255
1007	1008	Fe STIM	255
1009	1010	STIM error	255

Table 3.13: LET Science Data Frame, Range 4 (L3AL3B) Science/Foreground Rates, PENFGRATES

Frame Byte # (First)	Frame Byte # (Last)	Description	Particle ID
1011	1012	H (1.0-12.0 MeV/nuc)	0
1013	1014	H (12.0-15.0 MeV/nuc)	1
1015	1016	H (15.0-70.0 MeV/nuc)	2
1017	1018	He-4 (1.0-12.0 MeV/nuc)	3
1019	1020	He-4 (12.0-15.0 MeV/nuc)	4
1021	1022	He-4 (15.0-70.0 MeV/nuc)	5
1023	1024	C (1.0-21.0 MeV/nuc)	6
1025	1026	C (21.0-27.0 MeV/nuc)	7
1027	1028	C (27.0-33.0 MeV/nuc)	8
1029	1030	C (33.0-70.0 MeV/nuc)	9
1031	1032	N (1.0-21.0 MeV/nuc)	10
1033	1034	N (21.0-27.0 MeV/nuc)	11
1035	1036	N (27.0-33.0 MeV/nuc)	12
1037	1038	N (33.0-70.0 MeV/nuc)	13
1039	1040	O (1.0-27.0 MeV/nuc)	14
1041	1042	O (27.0-33.0 MeV/nuc)	15
1043	1044	O (33.0-70.0 MeV/nuc)	16
1045	1046	Ne (1.0-27.0 MeV/nuc)	17
1047	1048	Ne (27.0-33.0 MeV/nuc)	18
1049	1050	Ne (33.0-40.0 MeV/nuc)	19
1051	1052	Ne (40.0-70.0 MeV/nuc)	20
1053	1054	Mg (1.0-33.0 MeV/nuc)	21
1055	1056	Mg (33.0-40.0 MeV/nuc)	22
1057	1058	Mg (40.0-52.0 MeV/nuc)	23
1059	1060	Mg (52.0-70.0 MeV/nuc)	24
1061	1062	Si (1.0-33.0 MeV/nuc)	25
1063	1064	Si (33.0-40.0 MeV/nuc)	26
1065	1066	Si (40.0-52.0 MeV/nuc)	27
1067	1068	Si (52.0-70.0 MeV/nuc)	28
1069	1070	Fe (1.0-40.0 MeV/nuc)	29
1071	1072	Fe (40.0-52.0 MeV/nuc)	30
1073	1074	Fe (52.0-70.0 MeV/nuc)	31
1075	1076	He-3, Na, Al, S, Ar, Ca, Ni, Unidentified	255

Table 3.14: LET Science Data Frame, Range 4 (L3AL3B) Science/Background Rates, PENBGRATES

Frame Byte # (First)	Frame Byte # (Last)	Description	Particle ID
1077	1078	H Background	255
1079	1080	He Background	255
1081	1082	LiBeB Background	255
1083	1084	CNO Background	255
1085	1086	Z=9-30 Background	255
1087	1088	Z=30-40 Background	255
1089	1090	Z>=40 Background	255
1091	1092	Backward Background	255
1093	1094	H, He PEN	255
1095	1096	Z=3-30 PEN	255
1097	1098	Z>30 PEN	255

1099	1100	H, He STIM	255
1101	1102	CNO STIM	255
1103	1104	Fe STIM	255
1105	1106	STIM error	255

Table 3.15: LET Science Data Frame, Look Direction/Sectored Rates, SECTRATES

Frame Byte # (First)	Frame Byte # (Last)	# Bytes	Description
1107	1122	16	H, 4-6 MeV, Side A (Look Directions 0-7)
1123	1138	16	H, 4-6 MeV, Side B (Look Directions 8-15)
1139	1154	16	He-3, 4-6 MeV/nuc, Side A (Look Directions 0-7)
1155	1170	16	He-3, 4-6 MeV/nuc, Side B (Look Directions 8-15)
1171	1186	16	He-4, 4-6 MeV/nuc, Side A (Look Directions 0-7)
1187	1202	16	He-4, 4-6 MeV/nuc, Side B (Look Directions 8-15)
1203	1218	16	He-4, 6-12 MeV/nuc, Side A (Look Directions 0-7)
1219	1234	16	He-4, 6-12 MeV/nuc, Side B (Look Directions 8-15)
1235	1250	16	CNO, 4-6 MeV/nuc, Side A (Look Directions 0-7)
1251	1266	16	CNO, 4-6 MeV/nuc, Side B (Look Directions 8-15)
1267	1282	16	CNO, 6-12 MeV/nuc, Side A (Look Directions 0-7)
1283	1298	16	CNO, 6-12 MeV/nuc, Side B (Look Directions 8-15)
1299	1314	16	NeMgSi, 4-6 MeV/nuc, Side A (Look Directions 0-7)
1315	1330	16	NeMgSi, 4-6 MeV/nuc, Side B (Look Directions 8-15)
1331	1346	16	NeMgSi, 6-12 MeV/nuc, Side A (Look Directions 0-7)
1347	1362	16	NeMgSi, 6-12 MeV/nuc, Side B (Look Directions 8-15)
1363	1378	16	Fe, 4-6 MeV/nuc, Side A (Look Directions 0-7)
1379	1394	16	Fe, 4-6 MeV/nuc, Side B (Look Directions 8-15)
1395	1410	16	Fe, 6-12 MeV/nuc, Side A (Look Directions 0-7)
1411	1426	16	Fe, 6-12 MeV/nuc, Side B (Look Directions 8-15)

Table 3.16: LET Science Data Frame, Event Buffer

Frame Byte # (First)	Frame Byte # (Last)	Description
1427	1428	Event Buffer Header (# Event Records)
1429	4159	Event Records (filled as needed)

Appendix A: Rates Compression/Decompression Algorithm

The following algorithms were suggested in an e-mail from Don Reames, for compressing 32 bits to 16 bits. This finalized algorithm is a modified biased exponent, hidden one algorithm with a 12 bit mantissa and a 4 bit exponent. Numbers up to 2^{12} are uncompressed, and numbers up to 2^{13} decompress with no "error".

```
/* Rewrite to allow flexible arrangements of bits. AWL 030909 */
unsigned int      num_bits=16, num_mantissa_bits=12, num_exponent_bits=4;
unsigned long     output_mask=0xffff; /* 0xffff 16 bit, 0x0fff 12 bit */

/* 32-bit -> 16-bit compression for SW and HW rates     */
/* useage: rateout=pack_rate(ratein);              */

unsigned int pack_rate(ratein)
long ratein;
{
        unsigned int rateout, power=0;
        unsigned long mask;

        mask = (0xffffffff<<(num_mantissa_bits+1));
        while (ratein&mask)
        {
       power += (0x0001<<num_mantissa_bits);
       ratein>>=1;
        }
        rateout=ratein;
        if (power)
        {
                rateout = power + (0x0001<<num_mantissa_bits)
                        | (rateout & (output_mask>>num_exponent_bits));
        }

        rateout = (rateout & output_mask);

        return rateout;
}

/* Unpacking (not required in flight code) */
/* switched from long to unsigned long -- AWL 011107 */
unsigned long long_rate(packed) /* Unpack to long */
unsigned long packed;                   /* was just long.  AWL 030908 */
{
        unsigned long power;    /* was just long. AWL 030908 */
        unsigned long out; /* was just long.  AWL 030908 */

        power = packed>>num_mantissa_bits;
        if (power>1)
        {
                out = ( (packed & (output_mask>>num_exponent_bits))
                        | (0x0001<<num_mantissa_bits) );
                out = out<<(power-1);
        }
        else
                out = packed;
        return out;
}
```

```
double dbl_rate(packed) /* Unpack to double */
unsigned packed;
{
        int power;
        double out;

        power = packed>>num_mantissa_bits;
        if (power>1)
        {
                out = ( (packed & (output_mask>>num_exponent_bits))
                        | (0x0001<<num_mantissa_bits) );
                out = out * pow(2.,(double)(power-1));
        }
        else
                out = packed;
        return out;
}
```

Appendix B: LET Matrices

The LET Matrices are used in onboard processing for identifying particles by penetration range, element, and energy, using the delta–E vs. E' technique. The matrices and their use in the onboard software are documented elsewhere. However, for purposes of illustration, graphical representations of the matrices are included in this Appendix.

The matrices are 128 bins (x–axis) by 400 bins (y–axis), mapped over delta–E vs E' space. Each bin contains a number identifying either a "foreground" particle (selected elements or helium isotopes) or a "background" particle. Colors in the figures are assigned according to the bin value, but the colors are not unique to the bin values. Rather, light orange, red, and green were selected to contrast adjacent foreground tracks, and shades of blue and purple were selected to contrast adjacent background regions. The white (uncolored) region bounds backward–going particles, and STIM boxes are bright orange.

Solid yellow and dashed green lines center and outline the particle tracks for selected elements and helium isotopes. The curves were calculated using the Andersen and Ziegler (1977) range–energy relationship, assuming normal incidence through the LET detectors. The points are simulation data (M. Wiedenbeck, run 050).

The Matrices represented by the following plots are at Version 8e.

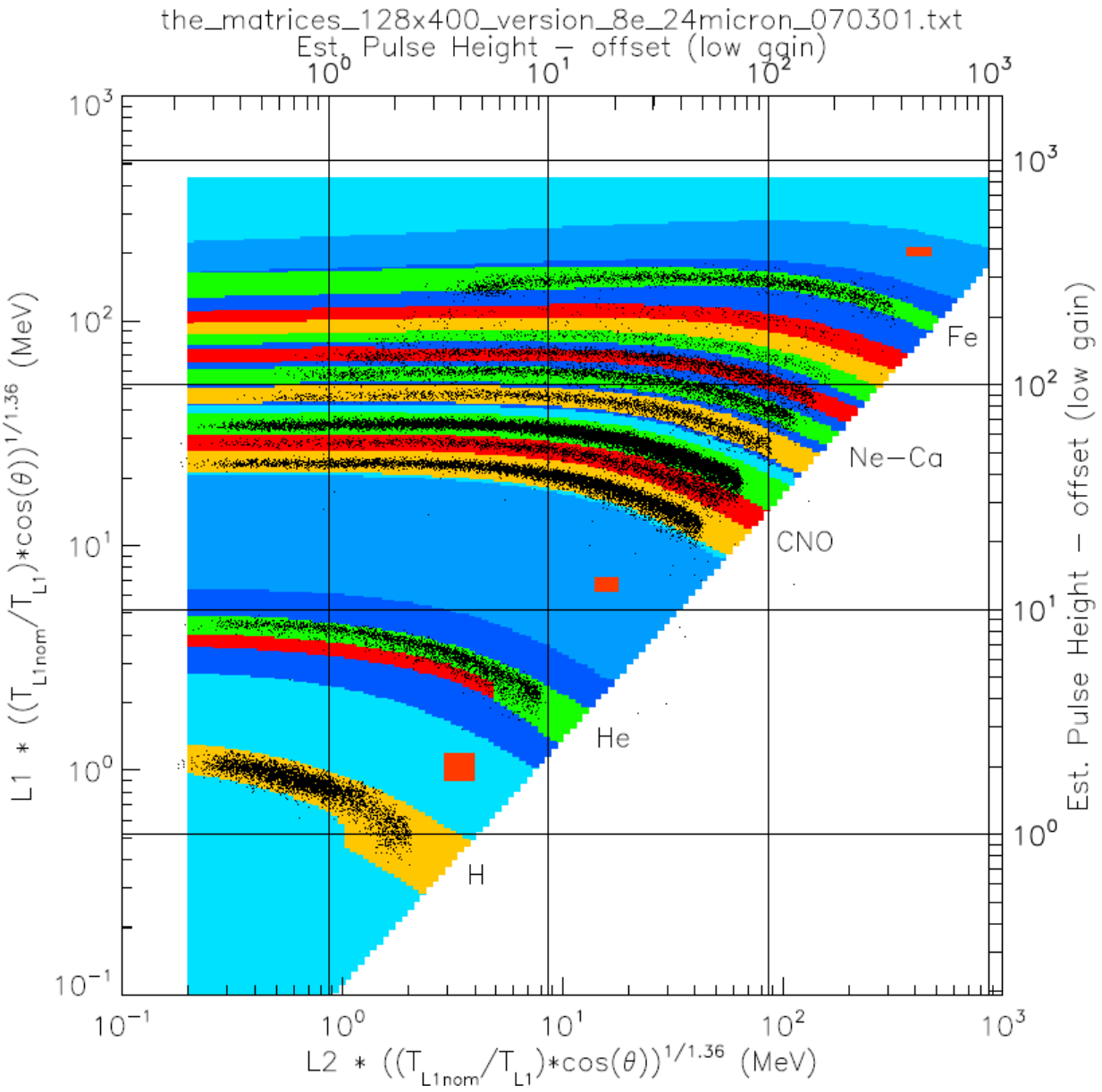

Figure C.1: The Range 2 (L1 vs. L2, or L1L2) LET matrix. Foreground elements are H, He-3, He-4, C, N, O, Ne, Mg, Si, S, Ar, Ca, and Fe.

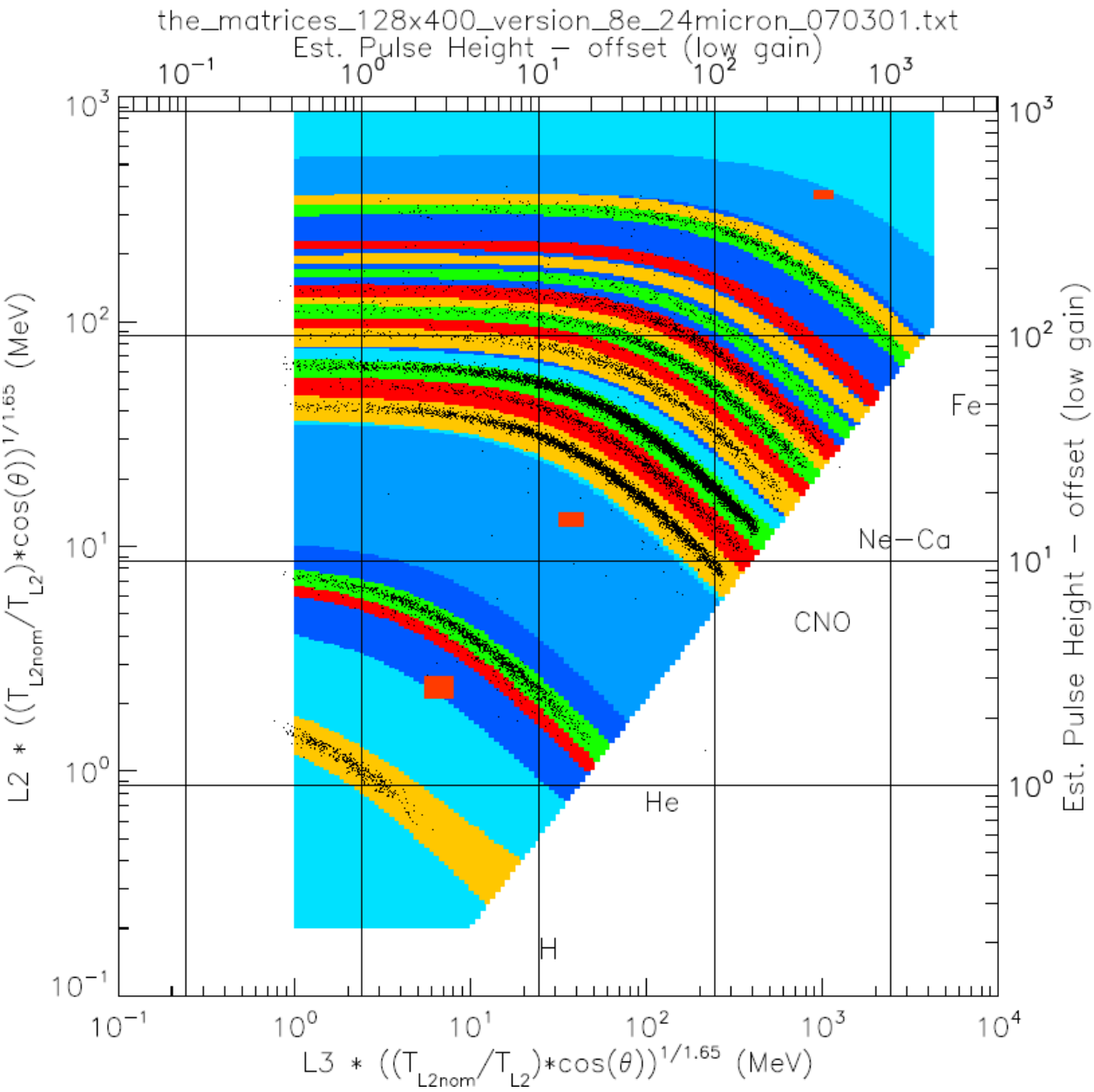

Figure C.2: The Range 3 (L2 vs. L3, or L2L3) LET matrix. Foreground elements are H, He-3, He-4, C, N, O, Ne, Na, Mg, Al, Si, S, Ar, Ca, Fe, and Ni.

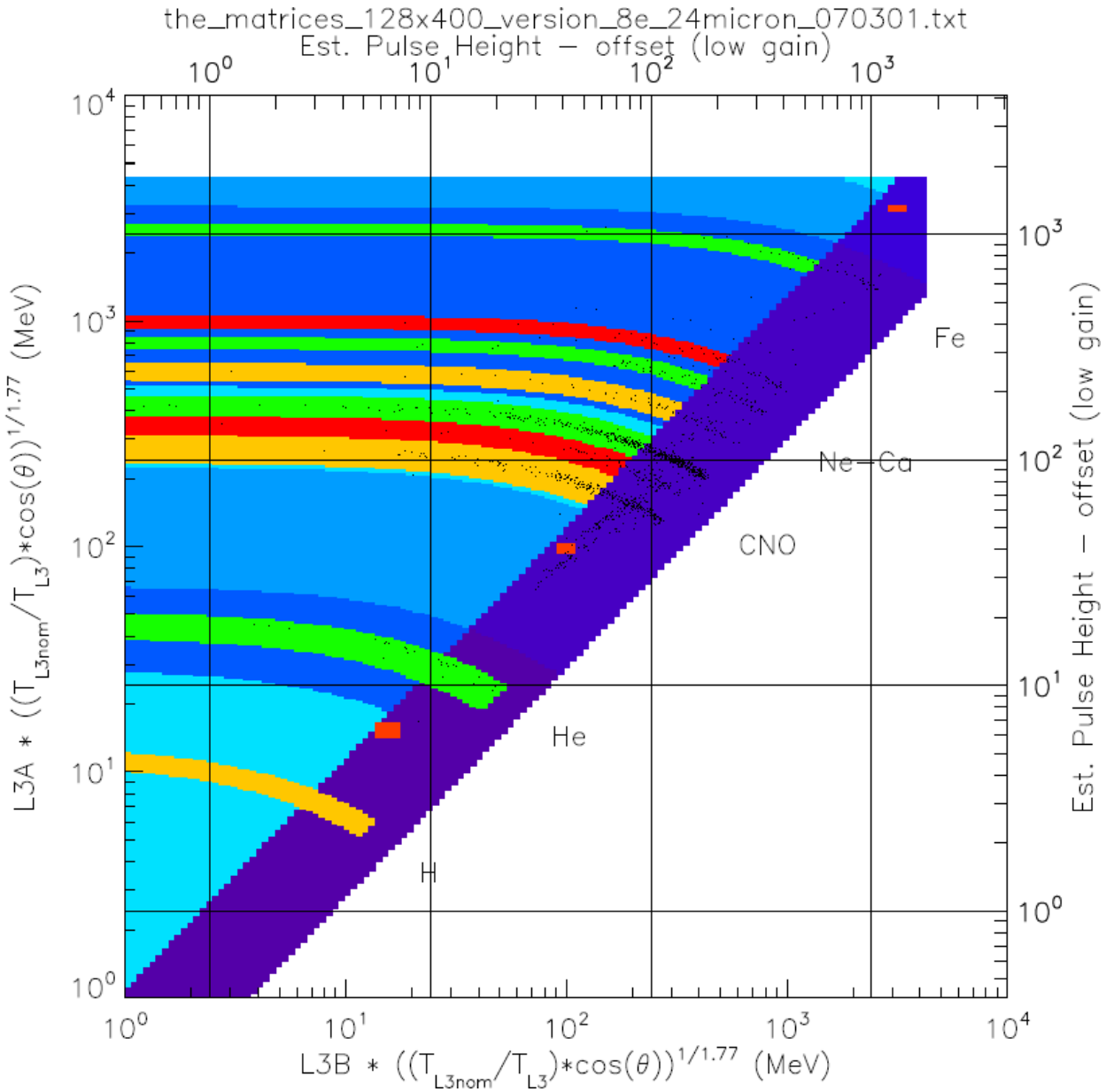

Figure C.3: The Range 4 (L3A vs. L3B, or L3AL3B) LET matrix. Foreground elements are H, He-4, C, N, O, Ne, Mg, Si, and Fe. The dark diagonal regions mark penetrating particles (or RNG 5).